Renewable Energy 224 (2024) 120111

Contents lists available at ScienceDirect

Renewable Energy

journal homepage: www.elsevier.com/locate/renene

Spatial analysis of renewable and excess heat potentials for climate-neutral district heating in Europe

Pia Manz [a,b,*], Anna Billerbeck [a,c], Ali Kök [d], Mostafa Fallahnejad [d], Tobias Fleiter [a], Lukas Kranzl [d], Sibylle Braungardt [e], Wolfgang Eichhammer [a,b]

[a] Fraunhofer Institute for Systems and Innovation Research, Breslauer Str. 48, 76139, Karlsruhe, Germany
[b] University Utrecht, Copernicus Institute of Sustainable Development, Princetonlaan 8a, 3584, Utrecht, the Netherlands
[c] University of Freiburg, Tennenbacher Str. 4, 79106, Freiburg, Germany
[d] Energy Economics Group, Technische Universität Wien, Karlsplatz 13, 1040, Vienna, Austria
[e] Oeko-Institut e.V., Merzhauser Str. 173, 79100, Freiburg, Germany

ARTICLE INFO

Original content: Spatial analysis of renewable and excess heat potentials for climate-neutral district heating in Europe (Original data)

Keywords:
District heating
Excess heat potentials
Renewable heat potentials
Clustering
Spatial analysis
Scenario analysis

ABSTRACT

District heating can play a decisive role in the transformation to a climate-neutral building sector, replacing fossil fuels. Renewable and excess heat potentials for district heating are often spatially limited and a consistent EU-wide analysis of the potentials is not yet available. In this paper, we quantify the renewable and excess heat potentials that could supply future district heating areas for the entire EU. We combine different data sets with a high spatial resolution and conduct spatial matching. Subsequently, we cluster the results for the potentials for individual district heating areas to derive representative types. The results show that the renewable and excess heat potentials together with heat pumps are overall sufficient to supply the future district heating demand, with high technical potentials from geothermal heat and excess heat from wastewater treatment plants. Decreasing the system temperatures increases the amount of available potentials. Lower heat densities and the overall character of the future supply sources require a paradigm shift in DH systems. Large central CHP units will need to be replaced by a diversity of several smaller sources, often combined with heat pumps and utilized at lower system temperatures.

1. Introduction and background

Decarbonised District Heating (DH) can be an important pillar for an efficient and climate-neutral heat supply for buildings, as various renewable and excess heat sources can be utilized, which was investigated by the Heat Roadmap Europe study [1], and can be cost-competitive, which was shown in an EU study [2]. Energy system analyses have modelled DH with different temporal and spatial resolutions, resulting in possible future DH market shares in the EU from 5% to 45% [3]. Especially regions with high heat demand DH are cost-competitive compared to individual heating systems.

In the future, there will be several challenges that need to be addressed in the field of DH. First, ambitious standards for the building stock are set by the EU legislative of the Energy Performance of Buildings Directive (EPBD) [4], leading to a reduced heat demand and, thus, possibly to a decreased competitiveness of DH due to lower heat sales. The competitiveness of DH depends not only on the supply costs but rather on the distribution costs, which decrease with increasing heat density, i.e. the heat demand per defined area. Several studies use empirical parameters to define the distribution costs and thus identify economic DH areas based on the heat density and effective width [5–11]. Second, renewable and excess heat should be the source for DH in a climate-neutral energy system. DH today mainly depends on heat from fossil-fuelled combined heat and power plants (CHP) [12], with fossil fuels contributing about 67% to the DH supply in the last years [13]. Consequently, the DH system itself needs to be transformed. One important measure is to decrease the supply temperatures of DH below 50 – 70 °C, into modern 4th and 5th generation DH networks, as investigated by several studies [14–18]. Many studies state the increased

* Corresponding author. Fraunhofer Institute for Systems and Innovation Research, Breslauer Str. 48, 76139 Karlsruhe, Germany.
E-mail addresses: pia.manz@isi.fraunhofer.de (P. Manz), anna.billerbeck@isi.fraunhofer.de (A. Billerbeck), koek@eeg.tuwien.ac.at (A. Kök), fallahnejad@eeg.tuwien.ac.at (M. Fallahnejad), tobias.fleiter@isi.fraunhofer.de (T. Fleiter), kranzl@eeg.tuwien.ac.at (L. Kranzl), s.braungardt@oeko.de (S. Braungardt), wolfgang.eichhammer@isi.fraunhofer.de (W. Eichhammer).

https://doi.org/10.1016/j.renene.2024.120111
Received 31 July 2023; Received in revised form 26 October 2023; Accepted 6 February 2024
Available online 10 February 2024

Abbreviations

CHP	combined heat and power
DH	district heating
EH	excess heat
EU	European Union with 27 member states
GHG	greenhouse gases
GIS	geographic information system
PyQGIS	QGIS python API
WtE	Waste-to-Energy
WWTP	wastewater treatment plants

efficient utilization of renewable or excess heat sources in low-temperature DH systems, especially in combination with heat pumps [19–23], as well as less heat losses and thus lower costs [24–28].

In general, several renewable and excess heat sources can be used for DH generation. Possible options are the direct use of renewable or excess heat sources and the use of low-temperature heat sources combined with heat pumps. Most of the potentials are limited by their spatial proximity to the DH demand, e.g. secondary biomass resources, geothermal, excess heat from industries (Industrial EH) and waste-to-energy plants (WtE), heat from surface water of rivers and lakes or wastewater treatment plants (WWTP). The suitability and high potential of renewable sources for heating has been proven in studies, e.g. shallow geothermal in the Canary Islands [29], Western Switzerland [30] and Vienna [31], deep geothermal in Geneva [32], the Himalaya region [33], biomass in rural areas in Spain [34], sea and river water heat pump in case studies in Norway [35] and Korea [36,37] as well as solar thermal in case studies in Northern EU [38] and Denmark [39]. However, all of these studies do not quantify potentials on a larger geographical scale. A high resolution of the input data sets is needed to quantify these potentials for DH, ideally georeferenced with coordinates. In some studies, potentials for renewable and excess heat sources for heating have already been allocated and quantified in a high resolution at the country- or EU-level, and several data sets are available, mainly focusing on technical potentials. Several studies have focused on the potentials for one individual country, e.g., for Italy [40], Germany [41,42] and Switzerland [43], while other country-level or EU-level studies have focused on individual technologies, considering potentials from e.g. geothermal [44–48], biomass [49,50], rivers and lakes [51,52], WWTP [53–56], industrial EH [57–60] and excess heat from WtE potentials [61–63]. Several open data sets are available for excess heat sources with the geographical extent of the EU, the Pan-European Thermal Atlas 5 (peta 5) [64], Hotmaps toolbox [65] and the Waste Heat Map [66].

Furthermore, DH supply potentials need to be analysed for each DH area (e.g. city or region with DH) to consider the local renewable and excess heat potentials. The method of allocating the demand and supply of heat with high spatial resolution is called spatial matching. Several studies analyse the spatial proximity of DH supply and demand, often focusing on one technology in one country. The matching algorithms use geographic information systems (GIS), either on proximity analysis enabling cost calculations [55,67–72] or spatial clustering with optimisation [73–76]. Several studies [47,54–57] introduced the terms supply or available potential in contrast to utilization or accessible potential, to differentiate the potentials of heat sources before and after spatial matching to the demand. Only one study matched the available renewable and excess heat potentials for DH in the geographical context of the EU with a high spatial resolution in the EU project sEEnergies [68]. However, it lacks a quantification of the renewable potentials on the country-level as well as potentials from rivers and lakes. Thus, there exists not yet a quantification of the technical renewable and excess heat potentials available for DH with high spatial resolution in the future. With this paper, we aim to fill this literature gap.

The quantification of heat generation potentials for DH on a regional level and the identification of DH types can be used to assess the future DH generation mix on EU-level, e.g. in district heating or energy system models and thus the economic potential of each source. In order to reduce the complexity of the results and analyse DH areas by their main potentials, the DH areas are clustered. With that, detailed results can be generalised, structured and understood, as well as serve as a basis for stronger conclusions for policy-making [77].

The objective of this paper is the quantification of the spatially limited renewable and excess heat potentials for DH by developing a spatial matching algorithm and clustering method. More specifically, we aim to answer the following research questions:

- How much can technical renewable and excess heat potentials in the EU contribute to supply the buildings' DH demand in a climate-neutral energy system?
- What is the potential role of the individual renewable and excess heat sources?
- What is the effect of transitioning towards low-temperature DH on the utilization of renewable and excess heat potentials?
- Which clusters of DH areas represent the respective renewable and excess heat potentials?

In this study, we focus on the geographical context of the EU-27 and assume a climate-neutral energy system. Our analysis is conducted based on annual values. Using GIS, we identify and match renewable and excess heat sources to future DH areas with high spatial resolution. Additionally, a hierarchical clustering algorithm categorizes the DH areas into distinct DH types based on their possible utilization of renewable and excess heat sources.

The structure of the paper is as follows: Chapter 2 describes the data used for quantifying renewable and excess heat potentials, along with a detailed description of the spatial matching and cluster algorithm method. In Chapter 3, the results of the potentials as well as the resulting DH types are presented. Chapters 4 and 5 are dedicated to discuss the results and draw conclusions based on the obtained results.

2. Data and method

Fig. 1 shows a schematic overview of the workflow. Two main data sets were used: (1) renewable and excess heat potentials for DH, and (2) identified future DH areas. Both data sets have high spatial resolution and include mainly annual energy values. The data sets were constructed and processed in three methodological steps. Step 1, the estimation of the renewable and excess heat technical potentials; step 2, the spatial matching with future DH areas; and step 3, the clustering based on the potentials resulting in DH types for EU. The identified data and results are discussed in the context of a climate-neutral energy system in 2050. The methodology and data were partly established within the EU project "Renewable Heating and Cooling Pathways, Measures and Milestones for the implementation of the recast Renewable Energy Directive and full decarbonisation by 2050 (N° ENER C1 2019-482)" [78]. Preliminary results were previously presented as a case study for Germany in a conference paper [41]. The dataset of the DH areas is a shapefile, containing the future DH demand for each of the 5815 DH areas. In the scenario, an ambitious DH expansion and connection rates are assumed, increasing the DH demand from 506 to 631 TWh, even though the buildings demand decreases significantly due to renovation. Details of the methodology, assumptions and results for the future DH areas are described in Appendix A.

2.1. Definition of scenarios

We analysed two scenarios in this study that differed by the assumed DH system temperature level: (1) high-temperature scenario and (2) low-temperature scenario. The two different DH system temperature

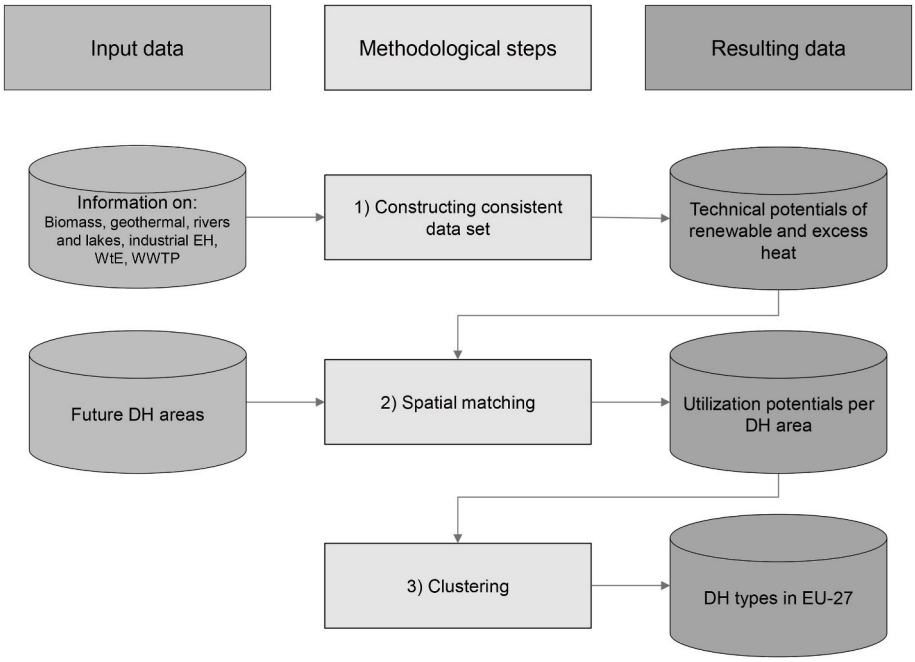

Fig. 1. Schematic overview of data input, methodology and results in this study.

levels were used to show the influence of temperature on the utilization of low-temperature heat sources and comprised the current level of 3rd generation DH (flow temperature 90 °C – 70 °C) and a lower temperature of 4th generation DH (flow temperature 60 °C – 70 °C). The DH demand in the DH areas is constant, with lower heat losses in the low-temperature scenario.

2.2. Definition of potentials

Generally, this study considers technical potentials and differentiates between supply and utilization potentials (see Fig. 2). In contrast, theoretical potentials represent the total heat that one resource could provide (e.g. the total amount of heat stored underground amounts to theoretical geothermal potentials). The technical potentials are limited by technical restrictions (e.g., the amount of heat that geothermal plants could extract). The supply potentials represent technical potentials limited by the geographical proximity to future DH areas (e.g. the geothermal plants that could be built close to a specific DH area). The method of spatial matching is used to identify the supply potentials. The utilization potentials represent technical potentials that are additionally limited by the DH demand in the DH areas that could utilize the potential (e.g. only the geothermal plants needed to serve the demand in the DH area are accounted for). For the technical potentials of rivers and lakes, additional economic limitations were considered in this study by assuming typical project sizes. The supply potentials and the DH demand are compared on an annual basis, and if the potential exceeds the demand, it is limited to the value of the annual DH demand. Thus, the seasonal match of heat demand and source load curves was only partly considered, mainly by assuming typical full-load hours for wastewater treatment and geothermal plants. The focus of this paper lies in the analysis of spatial proximity by spatial matching and identifying the utilization potentials.

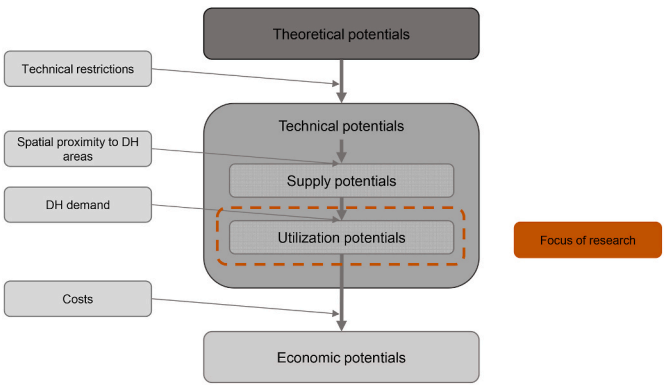

Fig. 2. Overview of type of potentials and each considered limiting factor.

2.3. Renewable and excess heat potentials

This section presents the data on the spatial availability of technical potentials suitable for DH generation and the assumptions and processing conducted to construct a consistent data set. We analysed the following heat supply sources: (1) Renewable sources, including deep geothermal, biomass and ambient heat from surface water and wastewater together with a heat pump as well as biogas from sewage sludge; (2) Excess heat from large industrial facilities and the thermal treatment of waste (WtE).

The data collection and processing steps depend on the technology and the available data. The technologies considered are summarized in Table 1, and the processing steps as well as assumptions are presented in the following subsections. The potential heat quantified in this paper always refers to the heat delivered to the DH area, i.e. after a heat pump for the heat from rivers and lakes and wastewater treatment plants (WWTP). An efficiency increase was assumed when systems temperatures are decreased, especially for heat pumps or CHP plants. The assumptions are also listed in the Table 1, showing the increase between the two temperature scenarios.

2.3.1. Biomass

In line with the EU ambitions on sustainable biomass, we assume a structural shift from primary biomass resources (e.g. round wood) to secondary sources for energy use [49,50]. The potentials for secondary sources will be shared for energy use in industry and the heating and DH sectors.

The biomass potentials were taken from the ENSPRESO data set

Table 1
Overview of the renewable and excess heat potentials considered.

Heat source	Spatial resolution (grid size)	Temporal resolution	Considered source temperature	Maximum distance from source, based on [25,71]	Source	Efficiency increase for low-temperature compared to high-temperature scenario, based on [79]
Biomass	NUTS 2	Annual	Direct combustion/ Biogas	Within NUTS 2	ENSPRESO - Biomass (JRC) [80]	Efficiency increases from 53% to 55% for biomass CHP
Geothermal (petro- and hydrothermal)	1000 × 1000 m	Annual, full-load hours considered	>60 °C	15 km	Geothermal Atlas [81], GeoDH [82]	No additional assumptions
Rivers and lakes	5000 × 5000 m	Annual, full-load hours considered	2–8 °C	5 km	Copernicus [83]	35% efficiency increase for heat pumps
Industrial excess heat	Coordinates	Annual, monthly profile considered	>55 °C	20 km	ISI Industrial Database [71]	Reduced recovery temperature
Waste-to-energy plants	Coordinates	Annual	100 °C	20 km	Peta 5 [64]	Efficiency increases from 66% to 76% for heat utilization
Wastewater treatment plants (heat and sludge)	Coordinates	Annual	10–25 °C	2 km	Peta 5 [64], Hotmaps [65]	33% efficiency increase for heat pumps. Efficiency increases from 50% to 55% for heat utilization of biogas CHP

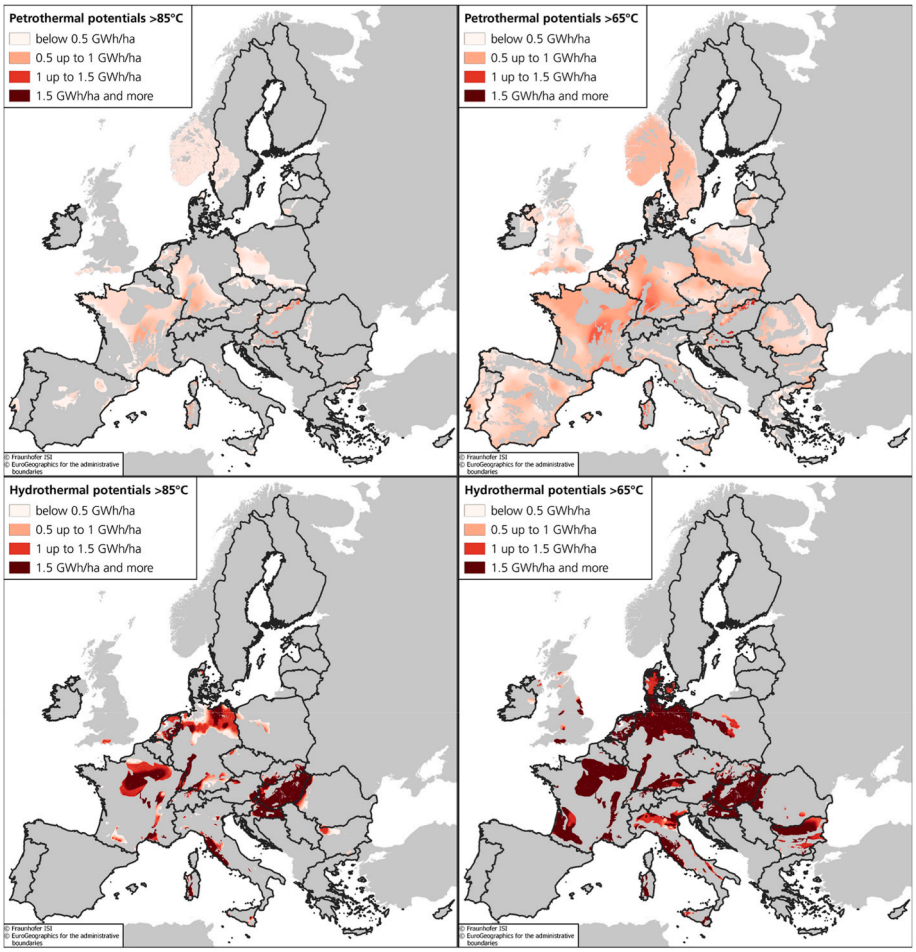

Fig. 3. Visualisation of the calculated annual technical geothermal potentials in the EU for petrothermal (top) and hydrothermal (bottom) in GWh per hectare. Possible areas with minimum temperatures for the high-temperature scenario (left) and the low-temperature scenario (right).

provided by JRC [80,84]. The data set is downloadable in tabular format, differentiated by commodity and at NUTS 2[1] level. We chose the annual values from the medium scenario (ENS_Med) for 2050 and selected residues from agriculture and forestry together with fast-growing energy crops.[2] With the additional assumption that 50% of these residues are available for DH, they represent an annual potential of

[1] NUTS (Nomenclature of Territorial Units for Statistics) regions is a hierarchical system used by the European Union (EU) for dividing up the territory of its member states for statistical purposes.

[2] The following codes represent the selected commodities: MINBIOAGRW1, MINBIOCRP31, MINBIOCRP41, MINBIOCRP41a, MINBIOFRSR1, MINBIOFRSR1a, MINBIOWOOW1, MINBIOWOOW1a.

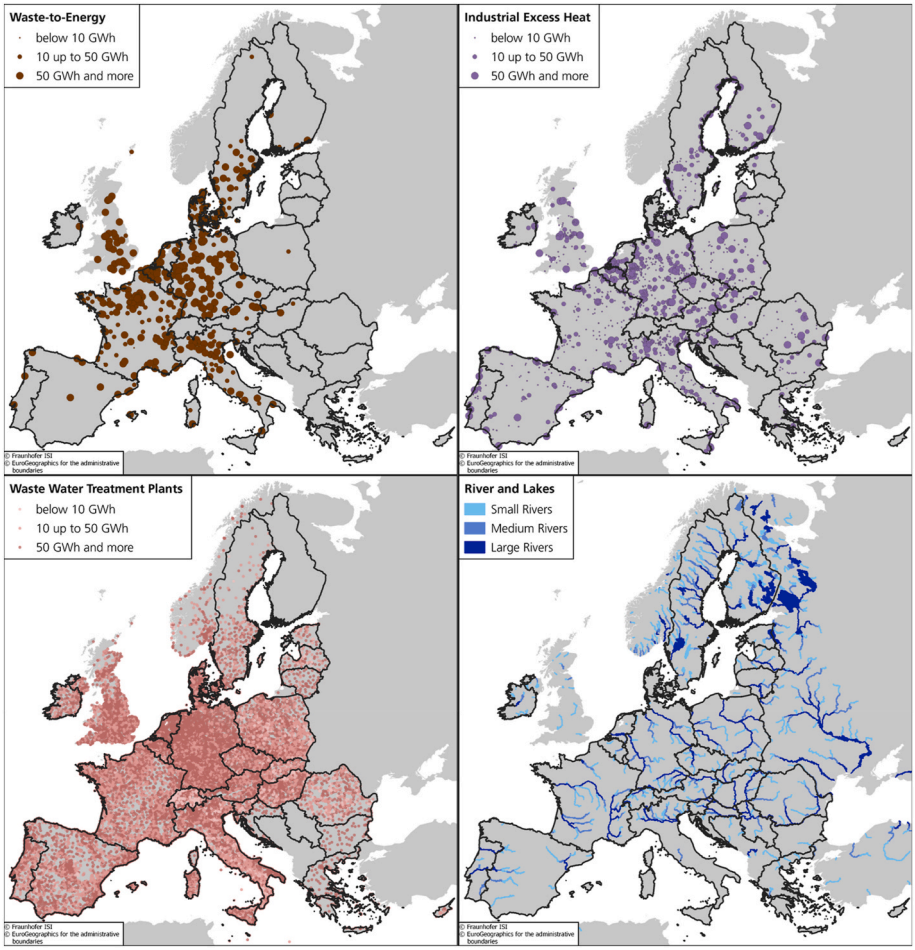

Fig. 4. Visualisation of the calculated annual technical potentials for renewable and excess heat potentials in the EU.

Table 2
Annual supply and utilization potentials for DH in a climate-neutral energy system in the EU, in TWh.

Heat source	High-temperature scenario			Low-temperature scenario		
	Technical potential	Supply potential	Utilization potential	Technical potential	Supply potential	Utilization potential
DH demand		732.13			694.26	
Biomass	727.86	727.86	385.30	742.41	742.41	377.16
Geothermal (hydrothermal)	814.94	422.89	80.12	2097.71	1201.36	173.84
Geothermal (petrothermal)	84.56	48.37	27.31	554.37	272.61	120.18
Rivers and lakes	1155.86	582.16	143.05	1553.48	782.42	153.58
of which electricity for heat pump	*428.10*	*215.62*	*52.98*	*427.83*	*215.48*	*42.30*
Industrial excess heat	19.91	19.52	16.19	32.48	31.96	29.88
Waste-to-Energy	97.91	97.14	88.16	110.63	106.85	95.49
Wastewater treatment plants	373.35	214.39	185.90	455.87	261.77	217.60
of which electricity for heat pump	*155.56*	*89.33*	*77.46*	*142.46*	*81.81*	*68.00*
Sludge	7.72	4.01	4.01	8.10	4.21	4.21
Total	3282.11	2116.34	930.04	5555.05	3403.61	1171.94

734 TWh for the EU. This biomass potential at NUTS 2 level was distributed to all DH areas in the respective NUTS 2 region, relative to the DH demand. This limitation implicitly assumes a short possible transport distance for secondary biomass.

2.3.2. Geothermal (hydro- and petrothermal)

In the EU, there were 2161 MW of geothermal plants for DH installed in 2020 [85], producing about 7.1 TWh of heat [86]. Geothermal plants consist of two (or more) boreholes, typically separated by a distance of around 1 km, one for extraction and one for injection of the fluid. In general, a distinction is made between petrothermal (i.e. hot dry rock, enhanced geothermal system) and hydrothermal (i.e. hot fluid) projects. Almost all the currently operating geothermal projects are hydrothermal plants that extract heat from thermal water in hot water basins and reservoirs at typical depths of 2000–4000 m. Petrothermal plants use the heat stored in underground rocks and extract it by injecting water as the extraction fluid. Generally, the petrothermal potential is by several factors higher than the hydrothermal potential, as the probability for the occurrence of water basins in the underground decreases with larger depths. Petrothermal projects have lower flow rates and thus lower economic competitiveness [87], despite recent advances in increasing the technical exploitation possibilities [88]. Competition for geothermal

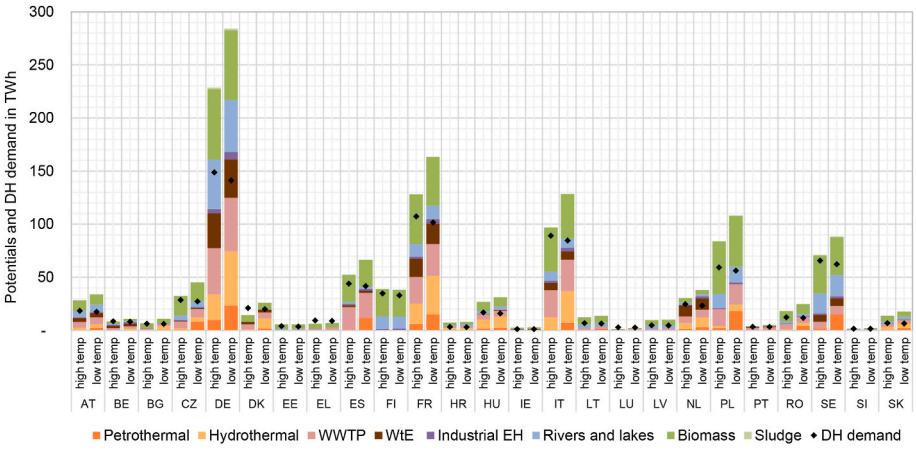

Fig. 5. Aggregated utilization potentials of renewables and excess heat for DH areas and DH demand in 2050 per country for the two scenarios.

Table 3
Overview of DH types for both scenarios with average share of the potentials to cover the demand (Note: Distinct patterns are shown in bold).

DH type	Total demand in TWh	Average demand in GWh	Number of DH areas	Petro-thermal	Hydro-thermal	WWTP	WtE	Industrial EH	Rivers and lakes	Biomass	Sludge
High-temperature scenario											
1	115	84	1364	14%	26%	31%	6%	2%	**99%**	74%	1%
2	32	44	714	24%	**98%**	**34%**	4%	5%	0%	72%	1%
3	542	198	2745	**4%**	**2%**	**18%**	**5%**	**6%**	**4%**	70%	0%
4	43	44	992	38%	1%	**73%**	0%	2%	0%	**74%**	1%
Low-temperature scenario[a]											
1	131	97	1346	40%	41%	35%	1%	3%	**98%**	77%	1%
2	87	60	1454	38%	**88%**	**38%**	1%	16%	5%	74%	1%
3	435	263	1652	**17%**	**8%**	**31%**	**16%**	**1%**	**6%**	67%	1%
4	42	31	1363	**98%**	1%	**44%**	0%	1%	0%	**78%**	1%

[a] When clustering the DH areas in the low-temperature scenario, the order of the clusters was changed, i.e. cluster 3 and cluster 4 were swapped. This was done in order to have the same sequence in both scenarios. This does not change the results but only the form of presentation.

Table 4
Qualitative description of the DH types for both scenarios.

DH type	Name	Description
1	Rivers and lakes	DH areas with high rivers and lakes potentials, supplemented by higher WWTP and hydrothermal potentials
2	Hydrothermal and WWTP	DH areas with high hydrothermal potentials, supplemented by higher WWTP and petrothermal potentials
3	Biomass	DH areas with overall lower (matched) potentials, except biomass
4	Mixed	DH areas with mixed potentials, especially petrothermal, WWTP and biomass

resources is not expected from individual heating systems, as these use near-surface geothermal energy. For geothermal projects, we assumed exploitation at depths between 2000 and 3000 m, with an underground temperature gradient of 30 K/1000 m [87]. In areas with hydrothermal potentials where high temperatures are available, geothermal plants can also operate as cogeneration units to produce heat and electricity. While this improves overall system efficiency, it also reduces the potential for DH supply. There may be other competing interests from land use (e.g. national parks, cities [89]) or mining activities (e.g. radioactive waste storage or carbon capture and storage [90]). Moreover, geothermal projects face high upfront costs and risks, as on-site test drillings are needed, which can reveal insufficient suitability (exploration risks).

We estimate the technical geothermal potentials based on two data sources: First, the Atlas of Geothermal Resources in Europe [81] provides maps for temperature contours at a depth of 2000 m. The data were extracted from the maps as raster files with a resolution of 1000 m × 1000 m. Each raster was assigned the respective temperature at 2000 m depth. This temperature was increased by 15 K, representing heat extraction between 2000 m and 3000 m. Second, the maps from the GeoDH project [82] were used to identify possible hydrothermal projects. From these, the areas classified as “hot sedimentary aquifer” and “other potential reservoirs” were extracted as vector layers for the 14 member states available. Other countries may also have hydrothermal potentials, however, no data is available. The temperature data were clipped to the vector layers, assuming that the temperature of the thermal fluid in the water basins is similar to the temperature of the rock. National parks and regions higher than 500 m above NN were excluded, as were water bodies. The geothermal potentials were quantified using the following formula, based on [87]:

$$P = Q{\cdot}\rho{\cdot}c{\cdot}(T_1 - T_2),$$

where T_1 is the underground temperature, and T_2 is the temperature of the injected water. As a volumetric flow rate Q was assumed, the density ρ and heat capacity c of water were used. Typical values were used for the flow rates with 0.0194 m^3/s for petrothermal projects [47,87] and 0.06 m^3/s for hydrothermal projects [48,87]. Potential areas were identified using a minimum temperature spread between T_1 and T_2 of 15 K, depending on the temperature scenario. For the extraction temperature, 85 °C was assumed for the high-temperature scenario and 65 °C for the low-temperature scenario. A risk factor was also included by assuming that 25% of hydrothermal and 50% of petrothermal projects are not successful [87]. Furthermore, 6.93 km^2 was assumed to be the area needed for one geothermal project with two boreholes. The potential P in MW was calculated for each raster in the map. Conservative values regarding the full load hours were assumed, 3000 and

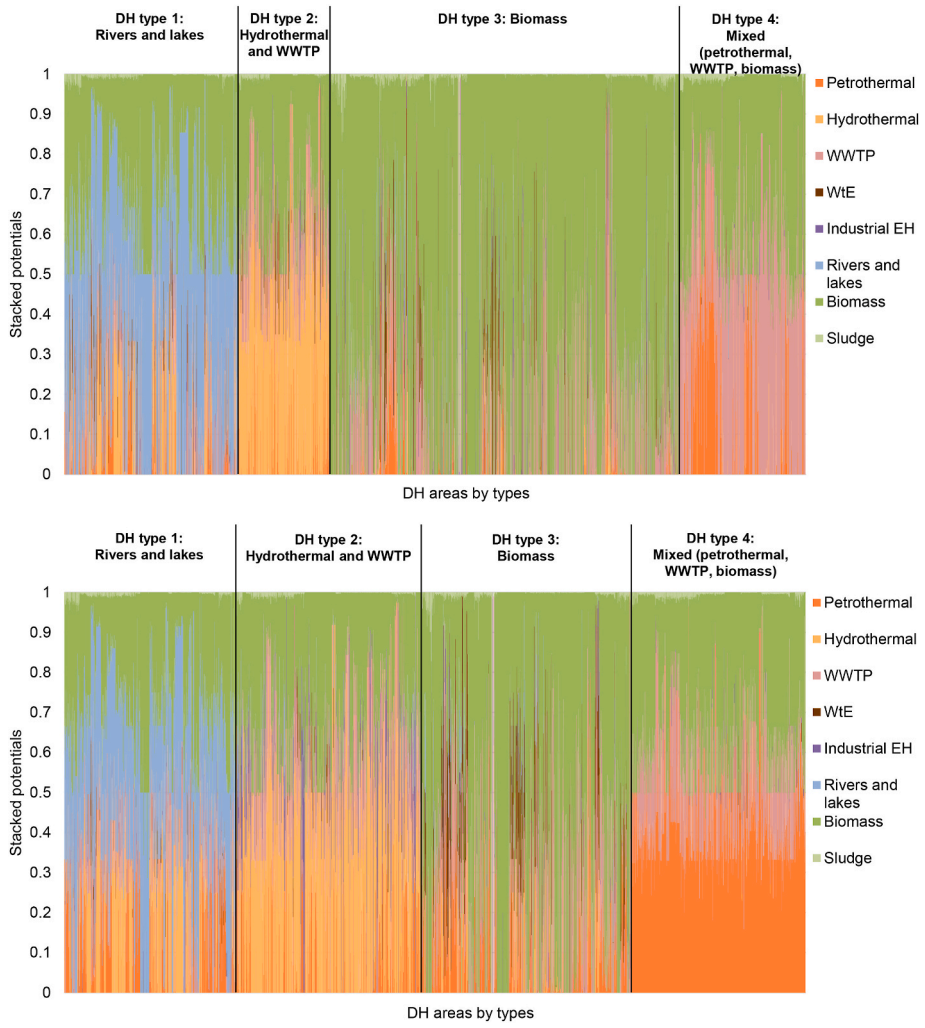

Fig. 6. Visualisation of the DH types in the high-temperature (top) and low-temperature (bottom) scenario.

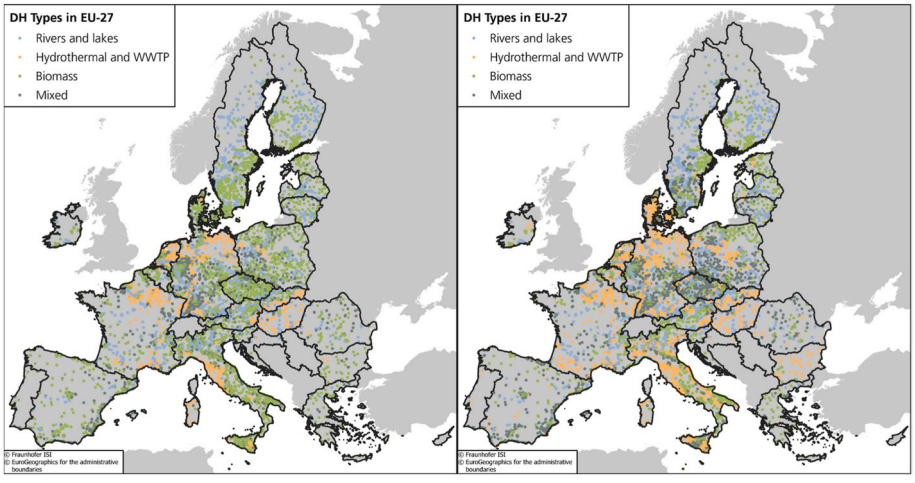

Fig. 7. DH areas in the EU identified by type in the high-temperature (left) and low-temperature (right) scenarios.

4000 full-load hours for petrothermal and hydrothermal projects [86,91], respectively, and were used to calculate the annual heat provided.

2.3.3. *Rivers and lakes*

Ambient heat from surface water like rivers and lakes can be a source for DH supply when combined with large-scale heat pumps [51,52,92]. Using water from rivers or lakes has implications for local ecosystems, such as a decrease in water temperature. However, this impact is marginal compared to conventional power plants that extract vast volumes of water for cooling and raise the temperature of rivers. Furthermore, heat pumps do not reduce the amount of water in rivers and lakes as it is returned after the heat has been extracted.

Table 5
Comparison of annual quantified potentials in literature with values identified in this study.

Heat source	Type of potential*	Geographical focus	Literature value in TWh	Value quantified in this study in TWh	Source
Biomass	Technical	EU	2300 (for all sectors)	734 (for DH)	Imperial College London [50]
Petrothermal	Supply	EU, 2050	1000 for buildings	273 (suitable with heat pump)	Dalla Longa et al., 2020 [46], based on [45]
Petrothermal	Technical	Germany	214–478	171–377	German Environment Agency [87]
Hydro- and petrothermal	Utilization	Germany	99 (of that mostly petrothermal)	34	TAB, 2003 [47]
Hydro- and petrothermal	Utilization	Austria, 2050	2–3	2	Könighofer et al., 2014 [48]
Hydrothermal	Utilization	Germany	300	24	Bracke et al., 2021 [44]
Rivers and lakes	Supply/ Utilization	Switzerland	44	Out of scope of the study	Gaudard et al., 2018 [52]
Waste-to-Energy (WtE)	Technical	EU, 2030	51	97	Persson & Münster, 2016 [62]
Waste-to-Energy (WtE)	Technical	Germany	30	35	Weber et al., 2020 [63]
Wastewater treatment plants (WWTP)	Supply	Hungary	0.2	5	Somogyi et al., 2020 [53]
Wastewater treatment plants (WWTP)	Utilization	Germany, 2050	37	43	Nielsen et al., 2020 [56]
Wastewater treatment plants (WWTP)	Utilization	Austria, 2050	0.5	6	Nielsen et al., 2020 [56]
Wastewater treatment plants (WWTP)	Utilization	Spain, 2050	16	21	Nielsen et al., 2020 [56]
Wastewater treatment plants (WWTP)	Utilization	France, 2050	18	25	Nielsen et al., 2020 [56]
Wastewater treatment plants (WWTP)	Utilization	BW in Germany, 2030	4	6	Münch et al., 2022 [54]

* The types of potential are defined in Section 2.2.

Detailed data on temperatures, flow rates and location in high temporal resolution is necessary to estimate the heat that could be extracted from rivers and lakes in the EU. A detailed and consistent data set is unavailable and has to be constructed. The data for river and lakes locations and monthly average flow rates were taken from Copernicus Climate Change Service Information [83]. Thereby, only rivers with a minimum average flow rate of at least 20 m^3/s in winter months were defined as suitable regarding temperatures, as lower flow rates lead to unsuitable temperatures [51]. The rivers and lakes were classified into three groups based on their average winter flow rate: (1) rivers with flow rates between 20 and 50 m^3/s were defined as small, (2) rivers with flow rates between 50 and 100 m^3/s as medium, and (3) rivers above 100 m^3/s as large. The temperatures were taken from hourly measurements from a data set published by the Federal State of Bavaria [93], grouped by the flow rates, and assigned to rivers throughout the EU. Typical project sizes were defined for each group (30 MW for small, 80 MW for medium and 150 MW for large projects, in combination with a heat pump) based on [51,94]. Full-load hours of 2000 h were assumed for smaller projects and 3000 h for medium and large projects so that we could estimate the annual amount of energy extracted from rivers and lakes using heat pumps. To estimate the electricity needed for DH supply, we assumed a seasonal performance factor for the heat pumps of 2.4 and 3.2 for the high-temperature and the low-temperature scenario, respectively. The minimum distance between two extraction points in the rivers was assumed to be 10 km [95].

2.3.4. Industrial excess heat (industrial EH)

Energy-intensive industries use large amounts of process heat, often at high temperature levels above 500 °C. Thus, excess heat potentials from large industrial plants are a promising source for DH. In the future, the amount of industrial excess heat available may decrease due to efficiency improvements in industrial processes and internal on-site heat utilization. We, therefore, assumed a reduction in industrial excess heat compared to today's potential based on [57]. In Ref. [57], excess heat from steel, cement, glass, paper, chlorine, ammonia, and methanol production was georeferenced in the ISI Industrial Database [96], and the effect of industrial transformation was estimated. The available industrial excess heat in 2050 was determined by considering the transformation of industry in terms of production volumes and low-carbon processes. This approach results in lower potentials, as improved energy and material efficiency lead to reduced production volumes. Electrified furnaces are often more efficient than conventional fossil fuel-based processes, which reduces not only energy demand but also excess heat potentials. The locations of industrial sites are assumed to remain unchanged. The methodology for estimating excess heat potentials based on production is described in Refs. [57,71] and has been adapted to include climate-neutral processes such as hydrogen-based steelmaking and petrochemical products. The flow temperature of DH systems also affects the energy available at industrial sites and is varied from 95 °C to 55 °C depending on the scenario.

2.3.5. Waste-to-energy (WtE)

Municipal solid waste is treated either by recycling, incineration or landfilling. Waste incineration plants (Waste-to-Energy, WtE) recover the energy that is contained in the treated waste, mainly by CHP [63]. The future potential of WtE is uncertain as it could be higher or lower than today's level, depending on the development of landfilling and circular economy approaches. There are implicit incentives for burning waste instead of reducing it once a WtE plant is built, as waste burning requires certain temperatures that are only reached at full capacity. This could lead to a stable amount of incinerated waste.

The sites and amount of the theoretically available excess heat (60% of energy input) from WtE plants were taken from the Pan-European Thermal Atlas 5 (peta 5) [64] as shapefiles, developed in the project Heat Roadmap Europe 4 [67]. From this, the heat recovery efficiency in CHP plants was assumed to reach 66% and 76% for the two temperatures respectively [62,97]. Further, we assumed that the locations and the amount of incinerated waste remain constant until 2050.

2.3.6. Wastewater treatment plants (WWTP)

Wastewater treatment plants (WWTP) are distributed all over the EU, often close to settlements. There is a regular inflow of sewage water and precipitation. The temperature remains relatively stable between 8 and 15 °C [53,56] and the heat contained could be used for DH when combined with a heat pump. There are a number of existing projects, e.g. in Budapest and Kalundborg, as well as the biggest project so far currently being built in Vienna.

We combined two data sources: Hotmaps [65,98] provides

calculated power of the plants, derived from the volume of sewage water and the temperature difference of 5 K. In peta 5 data and locations of annual excess heat from WWTP is published [64], taken from ReUseHeat [55]. As the Hotmaps dataset includes more plants, the locations and power values were taken from Hotmaps. The ReUseHeat dataset was used to derive typical full-load hours of 4421 by calculating average values for each plant where both power and annual excess heat were available. The seasonal performance factor of the heat pumps was assumed to be 2.7 and 3.6 for the high-temperature and the low-temperature scenario, respectively.

Additionally, sewage sludge can be fermented in an anaerobic digester to produce biogas (as is the case, for example, in Innsbruck and Amsterdam), often combined with solid waste. We used the sludge values from the ENSPRESO data set [80] and assigned them to the WWTP locations relative to size. Sewage sludge is often used in clinker production (kilns), and this may increase in the future, reducing the potential for DH generation.

2.3.7. Other potentials

We did not integrate any solar thermal potentials, as it was assumed that the technical potentials are not limited by the spatial proximity but rather the economic potentials limited by their costs. Technically, solar thermal can be utilized (almost) everywhere, as radiation is high enough in the EU [99]. Other types of heat pumps, e.g. air source heat pumps, were not considered for similar reasons. Furthermore, seasonal storage and peak load plants like hydrogen boilers, electric boilers or CHP plants were not considered, as they were not relevant to the research question of this paper.

2.4. Spatial matching

The regional analysis and spatial matching to the heat sources were conducted using a customized matching algorithm in the software QGIS with the PyQGIS plugin [100] mainly based on distance analyses. The renewable and excess heat potentials were matched to the most suitable DH areas identified within a defined maximum distance. The PyQGIS plugin allows the creation of Python scripts for automatized spatial data processing. Input data included future DH areas as polygons (see Appendix A) and the excess heat sources as point layers. The potential of geothermal and rivers and lakes had to be converted from raster to point sources, each point representing the potential of one geothermal project or river extraction point, with a minimum distance between each of them.

In the matching algorithm, which has previously been described in Ref. [57], the heat sources are allocated to the DH areas that are no further away than the assumed maximum distance. First, a spatial grid is created to pre-sort the heat sources to the DH areas, in order to reduce the calculation time by several factors. The DH areas within the distance limit are identified for each heat source. For industrial excess heat and WtE plants, the available energy is prioritized and sequenced by a calculated factor for each DH area within the maximum distance, based on its annual DH demand and the respective distance. This prioritization factor is used to allocate each excess heat source to one or several most suitable DH areas and prevents the connection of an industrial site with large amounts of excess heat to the closest but very small DH area. The prioritization factor also enables one individual large point source to supply multiple DH areas, e.g., multiple DH areas could be supplied by one WtE plant if the DH demand of one DH area is lower than the heat potential. Likewise, the prioritization factor is used to determine the order of multiple heat sources that could supply DH areas, with the source with the highest factor given priority, ensuring that large DH areas are supplied first. With that, a stepwise matching is conducted, with the largest DH areas being connected first until their demand could be supplied.

The output of the matching algorithm is a table with the matched potentials for each DH area, i.e. the supply potentials. These potentials are then used to calculate the utilization potentials by limiting the supply potentials to the magnitude of the annual DH demand in the matched DH area, which then forms the input for the clustering algorithm.

2.5. Clustering

A clustering analysis is performed as the final step to derive DH types, which we define as a set of DH areas with similar renewable and excess heat potential patterns. In line with this definition, input data for the clustering are the 5815 DH areas and their matched renewable and excess heat utilization potentials. In order to minimize the effect of different orders of magnitude, the potentials are expressed as a percentage of demand. This results in figures between 0 and 1, i.e. 0% – 100% coverage of the demand by a potential heat source.

Clustering was performed using an agglomerative clustering algorithm provided by the Python package SciPy.[3] In agglomerative clustering, the algorithm calculates the dissimilarity between all elements and gradually combines two elements with the least dissimilarity to form a cluster. This cluster is then reused in the next iteration. There are different algorithms varying in how they calculate the dissimilarity between the original elements and how the clusters are formed. In this paper, we use ward's minimum variance method and the Euclidean distance (similar to the analysis in Ref. [77]), as this best fits our data and objective. Further details on the clustering analysis, including a sensitivity analysis and the reasoning for our choice of algorithm, are provided in Appendix B.

3. Results

This chapter presents and analyses the renewable and excess heat potentials (first as technical potentials, then as supply and utilization potentials) in the EU. The final section presents the DH types identified by clustering the results for individual future DH areas.

3.1. Technical potentials

This section presents the technical potentials for renewable and excess heat sources in the EU with high spatial resolution. The identified geothermal potentials are classified into hydro- and petrothermal potentials for the two DH system temperatures assumed (Fig. 3). This means that the minimum underground temperature needs to be at least 85 °C for the high-temperature scenario and 65 °C for the low-temperature scenario. Petrothermal potentials are available across most countries in the EU but with lower heat extraction. This is mainly due to the lower flow rates assumed for petrothermal projects. Hydrothermal potentials, on the other hand, are more limited as they depend on the existence of aquifers but offer high local potentials. The DH system temperature and thus the return temperature strongly influence the availability and amount of the technical geothermal potentials.

The other potentials are more scattered over the countries with different spatial patterns (Fig. 4). Waste-to-Energy and industrial excess heat potentials comprise relatively large sources at fewer sites across the EU. In contrast to this, WWTPs are more widespread but with lower potentials. Potentials from rivers and lakes are limited to rivers with sufficient flow rates, which are generally larger rivers closer to the sea.

3.2. Supply and utilization potentials

The supply potentials are matched to future DH areas within the maximum distance, while the utilization potential comprises the demand that actually exists within the assumed distance. As this is calculated for each individual heat source, the sum of all source types can still

[3] https://docs.scipy.org/doc/scipy/index.html.

exceed the DH demand in the DH areas. Table 2 lists the technical, supply and utilization potentials, which are published per DH area in the online data repository [101]. The analysis includes the electricity demand for the heat pumps used in WWTP and rivers and lakes and is listed separately in Table 2. As the potentials can supply a considerable share of DH demand, the corresponding electricity demand is relatively high, even higher than some of the other potentials themselves. As a lower system temperature increases the efficiency of a heat pump, the electricity demand decreases in the low-temperature scenario, i.e., the same amount of heat could be provided to the DH area by using less electrical energy.

In general, the highest supply potentials are found in hydrothermal, biomass and wastewater treatment plants, depending on the assumed temperature level. The total utilization potential is several factors smaller than the supply potentials. This is mainly due to the high hydrothermal supply potentials in the EU, especially for the low-temperature scenario, greatly exceeding the DH demand. The heat from rivers and lakes shows a similar pattern to hydrothermal potentials but with a smaller increase due to lower system temperatures. In contrast to this, almost the entire potential from WWTP can be utilized, as these are often smaller plants close to larger cities with high DH demand. About 50% of the biomass supply potentials can be utilized if no transport across NUTS 2 regions is assumed. Overall, the calculated potentials are sufficient to supply the heat for DH demand in both scenarios at EU-level, with a higher potential in the low-temperature scenario. The aggregated utilization potentials at country level are sufficient to meet the DH demand in most countries (Fig. 5). At the level of individual DH areas, 128 TWh (17% of the total DH demand) in the high-temperature scenario and 66 TWh (9% of the total DH demand) in the low-temperature scenario cannot be covered annually. These figures do not include potential heat generation from solar thermal plants, air source heat pumps, or peak load boilers. Thus, overall there are enough renewable and excess heat potentials to reach a climate-neutral DH supply in 2050.

Reducing the system temperature from the high-temperature scenario to the low-temperature scenario can increase the potentials by 26%, mainly due to the broader availability of hydrothermal and petrothermal resources, as well as the improved efficiency of heat pumps using rivers and lakes and wastewater treatment plants as source. There is only a minor effect of the increased efficiency of heat utilization from WtE, industrial EH and biomass.

Where available, hydrothermal potentials could cover the main share of the DH supply. Furthermore, the dependency on biomass as a resource for DH generation could be reduced by lowering the DH system temperature. The other renewable and excess heat potentials could also cover a large share of the demand.

3.3. DH types

After quantifying the potentials, a clustering approach is used to define DH types. The DH types represent future DH areas with similar patterns of the available renewable and excess heat potentials (compare section 2.5 and Appendix B). In both scenarios, four different DH types were identified, although not all countries necessarily feature all four types. The dendrograms of the hierarchical clustering can be found in Appendix B.

Table 3 gives an overview of the four DH types with the average contribution of the potentials. Hence, beside the total and average DH demand per cluster, the average contribution of the different heat sources in percentage is shown, e.g. in cluster 1 in the high temperature scenario, 14% of the DH demand could be covered by petrothermal energy. In both scenarios and all DH types, biomass potentials are relatively high, and sludge potentials are relatively low as well as several renewable and excess heat sources can be used to cover the demand, i.e., all DH types represent multivalent networks.

The clusters show distinct patterns in both temperature scenarios. Cluster 1 can be supplied almost completely with heat from rivers and lakes, while representing quite low geothermal potentials. Cluster 2 shows the highest hydrothermal potentials, supplemented with high WWTP potentials. Cluster 3 has overall quite low potentials, except biomass potentials. Cluster 4 shows an overall more mixed pattern with dominant sources from petrothermal, WWTP and biomass, with a lower contribution of petrothermal in the high-temperature scenario. Even though the absolute contribution of the individual heat sources differs, from a qualitative point of view, the DH types in the two scenarios show several similarities, hence the clusters are given the same name (compare Table 4).

Fig. 6 further illustrates the DH types by showing the stacked potentials for all DH areas ordered by type, i.e., the DH areas are arranged on the x-axis and the potentials to cover demand are stacked on the y-axis. These figures further highlight the differences between the two scenarios. In the high-temperature scenario, a high number of areas are clustered in the biomass type, while the low-temperature scenario shows a more even distribution. Furthermore, in the low-temperature scenario, almost all areas can rely on a greater variety of sources. The reason for both these differences is that sources other than biomass are available to meet demand in the low-temperature scenario.

Not every country has all four DH types. For example, in the high-temperature scenario, Finland only has types 1 and 3: the rivers and lakes and the biomass type. These types represent the primary heat sources, but not the only ones. Thus, more sources are available in Finland than biomass and heat from rivers and lakes. More country-specific results are presented in Appendix C and in the online data repository [101].

The geographical allocation of the DH types mainly follows the available potentials (compare Fig. 7), especially for hydrothermal and rivers and lakes. The biomass and mixed types are mostly found in regions without hydrothermal or river and lake potentials, more distributed in the high-temperature scenario. For the low-temperature scenario, the geothermal areas are much more prominent due to the greater availability of geothermal energy for lower temperatures. However, the overall pattern is similar to the high-temperature scenario.

The results of the cluster analysis have significant implications for assessing transformation pathways in countries and the EU regarding DH by providing valuable insights into the most important renewable and excess heat sources. Moreover, the results offer a streamlined approach as an input for modelling DH supply mixes, in the way that they enable the reduction of the complexity of integrated energy system models while retaining essential technological and spatial details. Specific transformation pathways can be modelled with the cluster results as an input by considering different DH types as representatives of numerous DH areas across the EU, enabling a more focused analysis within energy system models.

4. Discussion

In this paper, we quantified the available potential to for the heat supply of future climate-neutral DH in the EU. The results show that biomass and geothermal energy could contribute large shares, covering up to 40–50% of future ambitious DH demand. Other large sources include heat from rivers and lakes and WWTP that could be exploited using heat pumps. If locally available, there is a high potential of excess heat from industrial plants and waste incineration. Thereby, the DH system temperature strongly influences the geothermal potential, as a lower temperature can double the hydrothermal potential where available and increases the scope of petrothermal potentials. The matched potentials serve 83% – 91% of the total DH demand locally, depending on the temperature level. The gap could be filled by air source heat pumps, solar thermal or peak load boilers as sources for DH that were not considered in this paper. Overall, we show that climate-neutral DH in the EU is technically possible. If the DH demand is even more widespread in the future than assumed, the supply and utilization potentials also increase as more potentials are in spatial proximity of the demand.

The method of spatial matching yielded the utilization potentials concerning the local annual demand and supply as well as the maximum

distances depending on the heat quantity of the source. The subsequent clustering reveals that most future DH areas include several different renewable and excess heat sources with different load profiles (i.e. multivalent DH systems).

Comparing the quantified potentials in this study to other analyses shows that our results are mostly in the range of existing literature (compare Table 5). The table also shows the large range of literature values. For industrial excess heat, the validation is published in previous papers [57,71].

There may be barriers to the exploitation of technical potentials. Exploiting geothermal energy involves risks due to drilling, high upfront costs, low public acceptance and complex permit processes. Limited data availability requires on-site exploration by project developers. Policy support and regulations, such as guarantee funds, are possibly required to manage such risks. Utilizing the heat from WWTPs and rivers and lakes could be challenging regarding regulations and market maturity, and WWTP operators may have varying rules regarding the return temperature. Utilizing industrial excess heat requires bilateral contracts between DH operators and companies. Long-term availability, downtimes, decreased production capacities, and changes in plant efficiency or closures add uncertainties. Installing backup technologies can reduce competitiveness. Data availability, especially for non-energy-intensive industries, is low, and integration into local heat planning may be challenging. Obligations for companies to assess and publish their excess heat potentials could help to identify potentials. Competition for biomass as a resource is likely to increase in the future, so the future availability for DH is uncertain. Furthermore, in this modelling approach, it was assumed that future DH areas are defined only by the distribution costs, as these were used as input data. However, DH areas could also be installed in regions with higher distribution costs where suitable renewable and excess heat potentials are located, e.g. geothermal, industrial excess heat, data centres or electrolysers. Furthermore, the implementation of climate-neutral DH systems has positive system effects, e.g. on flexibility and the market value of renewables in the electricity system [102–106], and reducing the necessary grid expansion [107].

This paper made several assumptions regarding the EU-wide potentials, the most important of which are discussed in the following. The potential of Waste-to-Energy was quantified without assuming any structural changes regarding waste. The amount could increase (as landfilling needs to be phased out in eastern EU member states) or decrease (due to a more circular economy). The composition could be more bio-based (if petrochemicals are substituted), or locations could shift to other EU countries. Furthermore, the amount of sewage water could change in the future and affect the potential from WWTP. Only general assumptions were possible concerning geothermal potentials. Field drilling is essential and could lead to entirely different results regarding underground temperatures, the existence of aquifers for hydrothermal use, and actual flow rates. The geothermal potentials quantified in this study were made without a heat pump. Including heat pumps could increase potentials in size and availability, and lower depths would be necessary. Hydrothermal also offers potential for electricity generation in CHP plants (Kalina and ORC) if sources above 100 °C are available [48]. Generally, if electricity is generated with 10% efficiency [108,109], the hydrothermal potential could decrease by 5–8%. Additionally, the assumption of a maximum transportation distance for biomass within a NUTS 2 area is inconsistent, as the NUTS 2 areas vary widely in size across different countries. This represents a conservative approach, particularly in DH types with high biomass potentials, as biomass could be transported over a larger distance. Generally, the distance assumptions based on typical sizes of the different sources do not strongly influence the results in a certain range of assumptions. However, the results of spatial matching of supply and demand depend on the method used [74]. The seasonal variability of DH demand and some sources could decrease the technical potentials and require cost-effective seasonal storage solutions. For excess heat, the reduction of the potential of 30% by seasonal mismatch was quantified by Bühler et al., 2018 [72], and the increase by utilizing seasonal storages by 12% was quantified by Chambers et al., 2020 [110]. The costs of such storage systems are uncertain and may decrease substantially in the future. Other excess heat sources like non-energy-intensive industries, data centres, hospitals, metro stations or the cooling of office buildings were not considered due to missing data but could provide excess heat on a low-temperature level and could increase the efficiency of heat pumps compared to air-source heat pumps [56,111].

5. Conclusions

To reach climate-neutrality in 2050, DH must be based on renewables and excess heat. This paper quantifies the technical potentials of renewable and excess heat sources for future DH systems in 2050 for the geographical extent of the EU-27 and high spatial resolution.

The findings indicate that there is sufficient potential of renewable and excess heat sources to supply DH in the future even when DH is expanded to an ambitious market share of 33%. Both types of geothermal energy, hydrothermal and petrothermal, show large potentials in many countries. Hydrothermal energy is unevenly distributed across the EU and shows vast potentials in locations where it is available, particularly in Germany, Denmark, Hungary, Romania, and Slovakia. The supply potentials are several times higher than the DH demand close by. Petrothermal sources are available in many regions but come with inherent risks and low technological maturity. Furthermore, biomass from secondary sources such as residues has a high potential. Heat from Waste-to-Energy shows a high potential to supply DH. Industrial excess heat from large individual point sources represents a possibility for utilization, whereby the number and thus the amount of heat is smaller than of other sources. Heat pumps can utilize heat from wastewater treatment plants and rivers and lakes, having a potential distributed all over the EU. Furthermore, the results highlight that decreased system temperatures can increase the available technical potentials for DH by 26%. This is particularly relevant for geothermal potentials, which increase by a factor of three. This can substantially reduce the dependency on biomass. The exploitation of the available utilization potentials requires a paradigm shift, which involves a transition from large scale CHP units to a greater variety of smaller sources at lower temperatures, often combined with heat pumps.

Further research is needed to identify the economic potentials and thus hint to the future cost-optimal DH supply mix. Our study provides the basis to identify the local renewable and excess heat potentials that are spatially limited. The DH types defined here are published as open data set and can be used to model DH supply mixes and dispatch. Possible transformation paths can be modelled for the different representative DH types and thus reduce the complexity of energy system modelling.

Finally, this article provides combined and harmonised potentials for renewable and excess heat sources for district heating supply in 2050 for more than 5000 areas in Europe. This paper is the first to present potentials in high resolution for the future supply of DH, thus contributing significantly to improving the data situation, which can be used in future research. Finally, it emphasizes the need for strategic policies, coordination, and collaboration among various stakeholders to effectively exploit the potentials and drive the paradigm change towards sustainable DH systems.

CRediT authorship contribution statement

Pia Manz: Conceptualization, Data curation, Formal analysis, Investigation, Methodology, Software, Validation, Visualization, Writing – original draft, Writing – review & editing. **Anna Billerbeck:** Methodology, Software, Formal analysis, Investigation, Writing – original draft. **Ali Kök:** Methodology, Writing – review & editing. **Mostafa Fallahnejad:** Resources, Writing – review & editing. **Tobias Fleiter:** Validation, Writing – review & editing. **Lukas Kranzl:** Validation, Writing – review & editing. **Sibylle Braungardt:** Funding acquisition, Writing – review & editing. **Wolfgang Eichhammer:** Supervision.

Declaration of competing interest

The authors declare that they have no known competing financial interests or personal relationships that could have appeared to influence the work reported in this paper.

Data availability

Spatial analysis of renewable and excess heat potentials for climate-neutral district heating in Europe (Original data) (Fordatis)

Acknowledgements

The analysis is based on work conducted within the project "Renewable Heating and Cooling Pathways, Measures and Milestones for the Implementation of the Recast Renewable Energy Directive and Full Decarbonisation by 2050″ with the project reference number N° ENER C1 2019-482. The authors would like to thank all the project members, namely Oeko Institute, TU Vienna, e-think, Halmstad University and Fraunhofer ISI. Furthermore, we want to thank our student assistant Friedrich Graaf for his excellent work in developing the matching algorithm. The publication was supported by the Fraunhofer Cluster of Excellence "Integrated Energy Systems" (CINES).

During the preparation of this work the authors used ChatGPT 4 in order to improve readability and language checking. After using this tool, the authors reviewed and edited the content as needed and take full responsibility for the content of the publication.

Appendix

Appendix A. DH areas

This appendix provides a description of how the DH areas are modelled and where more information about the approach is published. To model the future location and extent of DH areas in the EU-27, the parameters of heat demand, gross floor area, a distribution cost ceiling and a DH market share within DH areas (connection rate) are set exogenously as input parameters to the calculation. The annual useful heat demand for residential and tertiary buildings in the EU is modelled to decrease from 3129 TWh in 2020 to 1900 TWh in 2050. This significant decrease of the heat demand leads to a decreased economic competitiveness of DH, which could be compensated with high connection rates. Therefore, it was assumed that in all countries, a connection rate between 70% and 90% within DH areas should be maintained or achieved till 2050. TableAnnex 1 shows the assumed DH connection rate and cost ceiling per country in 2020 and 2050. For the identification of the DH areas, two conditions should be fulfilled:

- The annual heat demand supplied in a DH area should be greater than 5 GWh/a;
- The average distribution cost may not exceed the pre-defined distribution cost ceiling.

A depreciation time of 40 years is considered for the DH grid. More about the modelling approach, assumptions and results can be found in the project report [78] as well as in Ref. [112] and a python implementation of the approach is provided on Github [113].

TableAnnex 1
Country-specific DH connection rate in 2020 and 2050 and distribution cost ceiling as input parameter.

Country[1]	DH connection rate, 2020	DH connection rate, 2050	Distribution cost ceiling, 2050 in €/MWh
AT	55%	80%	36
BE	15%	70%	34
BG	64%	75%	38
CZ	44%	80%	35
DE	32%	75%	36
DK	88%	90%	40
EE	58%	80%	36
EL	29%	70%	31
ES	3%	70%	36
FI	63%	90%	37
FR	15%	75%	41
HR	37%	80%	32
HU	33%	80%	30
IE	0%	70%	36
IT	17%	70%	36
LT	78%	90%	32
LU	29%	80%	32
LV	57%	80%	32
NL	26%	75%	38
PL	51%	80%	31
PT	33%	70%	41
RO	43%	75%	32
SE	86%	90%	42
SI	52%	80%	31
SK	74%	90%	32

[1] Please note, that Malta and Cyprus have no DH installed until 2050.

Two or more identified coherent DH grids are considered as one connected DH area, if their focal points lie in the same LAU 2[4] region. Distribution losses occur when the heat is transported through the pipe system, from the heat generation to the heat demand. Thus, 10% and 16% of the demand for

[4] LAU (Local Administrative Units) is a territorial classification system used by the European Union for statistical purposes. LAU divisions provide a more detailed breakdown of regions compared to the NUTS classification within member states.

the low- and high-temperature scenario respectively was added, before matching to possible heat sources.

The DH demand and connection rate change in the time horizon until 2050. The DH potential is obtained by multiplication of the heat demand in the identified DH areas with the country-specific connection rate. Based on the investment made for the DH distribution grid and delivered heat by DH from 2020 to 2050, the average cost of DH distribution per unit of delivered heat in each country is calculated.

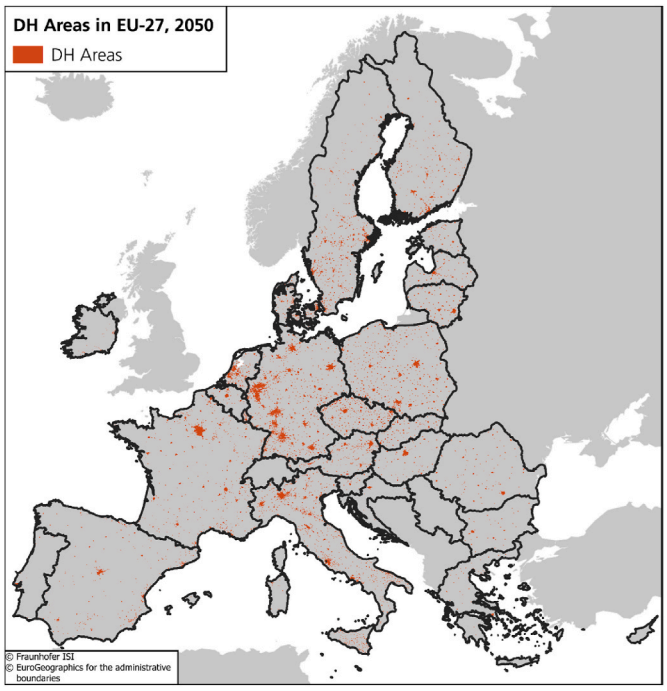

Fig. Annex 1. DH areas in the EU in 2050.

The resulting DH demand increases by 31.6%, from 506 TWh in 2020 to 631 TWh in the EU in 2050, with 5815 identified DH areas (FigureAnnex 1). An overview of the results of DH potentials per country in 2020 and 2050 is provided in TableAnnex 2. Average distribution costs of 31.4 €/MWh can be expected for EU. The average distribution costs in Netherlands and Portugal are relatively higher than in other countries. This is due to the fact that these countries have a low starting connection rate, leading to lower heat supply over the period of 2020–2050 and therefore, higher average distribution costs. Three countries, namely Estonia, Latvia and Lithuania, have relatively low average distribution cost as the heat density within DH areas in these countries is very high and the DH connection rate remains high through the study horizon.

TableAnnex 2
DH demand in DH areas modelled for 2020 and 2050 as well as key indicators comparing to total heat demand for buildings.

Country	Demand in DH areas in GWh		Heat demand covered by DH in %		Heat demand covered by DH in GWh		Average distribution costs in €/MWh
	2020	2050	2020	2050	2020	2050	
AT	38,763	19,890	25.3%	33.2%	21,319	15,912	28.1
BE	26,027	10,636	3.4%	14.1%	3904	7445	32.8
BG	10,160	7382	26.7%	34.9%	6503	5536	28.7
CZ	51,729	30,994	24.7%	43.0%	22,761	24,795	28.1
DE	375,321	171,208	14.9%	32.4%	120,103	128,406	33.0
DK	35,273	20,287	52.8%	46.7%	31,040	18,259	32.6
EE	9105	4293	42.1%	52.2%	5281	3434	14.3
EL	14,346	11,582	10.8%	24.8%	4160	8107	29.4
ES	65,881	54,311	1.4%	30.8%	1976	38,018	33.3
FI	57,870	33,453	47.6%	63.0%	36,458	30,108	30.5
FR	203,160	123,460	6.3%	27.5%	30,474	92,595	33.7
HR	7702	3614	11.3%	25.7%	2850	2892	31.9
HU	32,249	18,281	13.3%	32.5%	10,642	14,625	28.2
IE	1760	1630	0.0%	4.7%	0	1141	33.1
IT	178,312	109,970	7.9%	31.0%	30,313	76,979	33.8
LT	10,987	6625	49.2%	59.2%	8570	5962	15.9
LU	5266	3066	19.5%	51.7%	1527	2453	29.0
LV	11,195	5253	41.5%	59.9%	6381	4203	15.9
NL	46,759	28,372	9.0%	26.5%	12,157	21,279	35.7
PL	130,002	63,942	27.2%	38.0%	66,301	51,153	29.6
PT	5437	4390	6.4%	13.9%	1794	3073	40.5
RO	29,236	14,314	15.0%	26.0%	12,571	10,735	29.8
SE	66,416	62,989	66.3%	65.5%	57,118	56,690	30.7
SI	3192	1809	13.6%	19.2%	1660	1447	30.7
SK	13,582	6614	32.7%	36.9%	10,051	5952	29.4
EU	1,429,732	818,367	16.2%	33.2%	505,916	631,202	31.4

Appendix B. Cluster analysis

This appendix provides additional details on the cluster analysis, including a sensitivity analysis with different clustering algorithms. Clustering or cluster analyses is a collective term for statistical procedures that make it possible to structure a data set by group assignments. Cluster analyses are based on the consideration of the similarity or distance of the objects to each other. There are a variety of different algorithms that use different distance measures to assign objects to clusters. In general, partitioning (including k-means), hierarchical, density-based, grid-based and combined methods are distinguished (compare [114]).

In this paper, we performed hierarchical clustering as well as k-means clustering. In hierarchical clustering, the algorithm calculates the dissimilarity between all elements and gradually combines two elements with the least dissimilarity into a cluster. This formed cluster is then used again in the next iteration. In k-means clustering, clusters are represented by a central vector. When the number of clusters is fixed to k, k-means clustering gives a formal definition as an optimization problem: find the k cluster centres and assign the objects to the nearest cluster centre, such that the squared distances from the cluster are minimized. The hierarchical clustering was performed using algorithms provided by the Python package SciPy.[5] The k-means clustering was computed using the k-means++ algorithm provided by the Python package Scikit-learn.[6]

Input data for the clustering are the DH areas with their matched renewable and excess heat potentials. In order to minimize the effect of different orders of magnitudes, the potentials are expressed as a percentage of demand, resulting in figures between 0 and 1, i.e. 0%–100% coverage.

Thus, the following input figures are used in the clustering:

- Petrothermal potentials as a percentage of demand coverage [%],
- Hydrothermal potentials as a percentage of demand coverage [%],
- Potentials form WWTP a percentage of demand coverage [%],
- Potentials from WtE as a percentage of demand coverage [%],
- Industrial EH potentials as a percentage of demand coverage [%],
- Rivers and lakes potentials as a percentage of demand coverage [%],
- Biomass potentials as a percentage of demand coverage [%],
- Sludge potentials as a percentage of demand coverage [%].

TableAnnex 3 provides the maximum, the minimum and the mean of the input data per scenario.

TableAnnex 3
Overview of input data for the cluster algorithm.

Scenario	High temperatures			Low temperatures		
	Maximum	Minimum	Mean	Maximum	Minimum	Mean
Petrothermal	100%	0%	14.6%	100%	0%	46.5%
Hydrothermal	100%	0%	19.3%	100%	0%	34.0%
WWTP	100%	0%	32.5%	100%	0%	36.8%
WtE	100%	0%	4.6%	100%	0%	5.2%
Industrial EH	100%	0%	4.4%	100%	0%	5.3%
Rivers and lakes	100%	0%	25.2%	100%	0%	25.7%
Biomass	100%	0%	71.7%	100%	0%	73.5%
Sludge	8.5%	0%	0.8%	9.4%	0%	0.9%

B.1 High-temperature scenario

For the hierarchical clustering algorithms, we use the cophenetic correlation coefficient[7] to compare different linkage types and dissimilarity calculations (TableAnnex 4). This coefficient calculates the cophenetic distances between each observation in the hierarchical clustering defined by the linkage. It measures the height of the dendrogram at the point where two branches merge. The magnitude of this value should be close to one for a high-quality solution.

TableAnnex 4
Cophenetic correlation coefficient for different hierarchical clustering (S1).

metric	method					
	ward*	centroid*	single	complete	average	weighted
euclidean	**0.705**	**0.826**	0.590	0.787	**0.842**	0.797
cityblock (Manhattan distance)	–	–	0.524	0.604	0.826	0.759
mahalanobis	–	–	0.509	0.583	0.655	0.543
chebyshev	–	–	0.624	0.628	0.807	0.681

Note: Numbers in bold indicate which clusterings are selected for further analysis. *Ward and centroid require Euclidean distance.

[5] See https://docs.scipy.org/doc/scipy/reference/generated/scipy.cluster.hierarchy.linkage.html#scipy.cluster.hierarchy.-linkage and https://docs.scipy.org/doc/scipy/reference/generated/scipy.spatial.distance.pdist.html#scipy.spatial.distance.pdist.

[6] See https://scikit-learn.org/stable/modules/generated/sklearn.cluster.KMeans.html and https://scikit-learn.org/stable/modules/clustering.html#k-means.

[7] See https://docs.scipy.org/doc/scipy/reference/generated/scipy.cluster.hierarchy.cophenet.html.

For further analysis, we choose three hierarchical clusterings with a high cophenetic correlation coefficient. We also computed k-means clustering as an additional sensitivity. Thus, the following clusterings are analysed:

- S1.1: hierarchical clustering with average linkage and Euclidean distance,
- S1.2: hierarchical clustering with centroid linkage and Euclidean distance,
- S1.3: hierarchical clustering with ward linkage and Euclidean distance,
- S1.4: k-means clustering.

In hierarchical clustering, dendrograms, which show the pairwise combination of elements over dissimilarity, are used to select a terminus, i.e. the number of clusters. FigureAnnex 2 shows the dendrograms of the hierarchical clusterings.

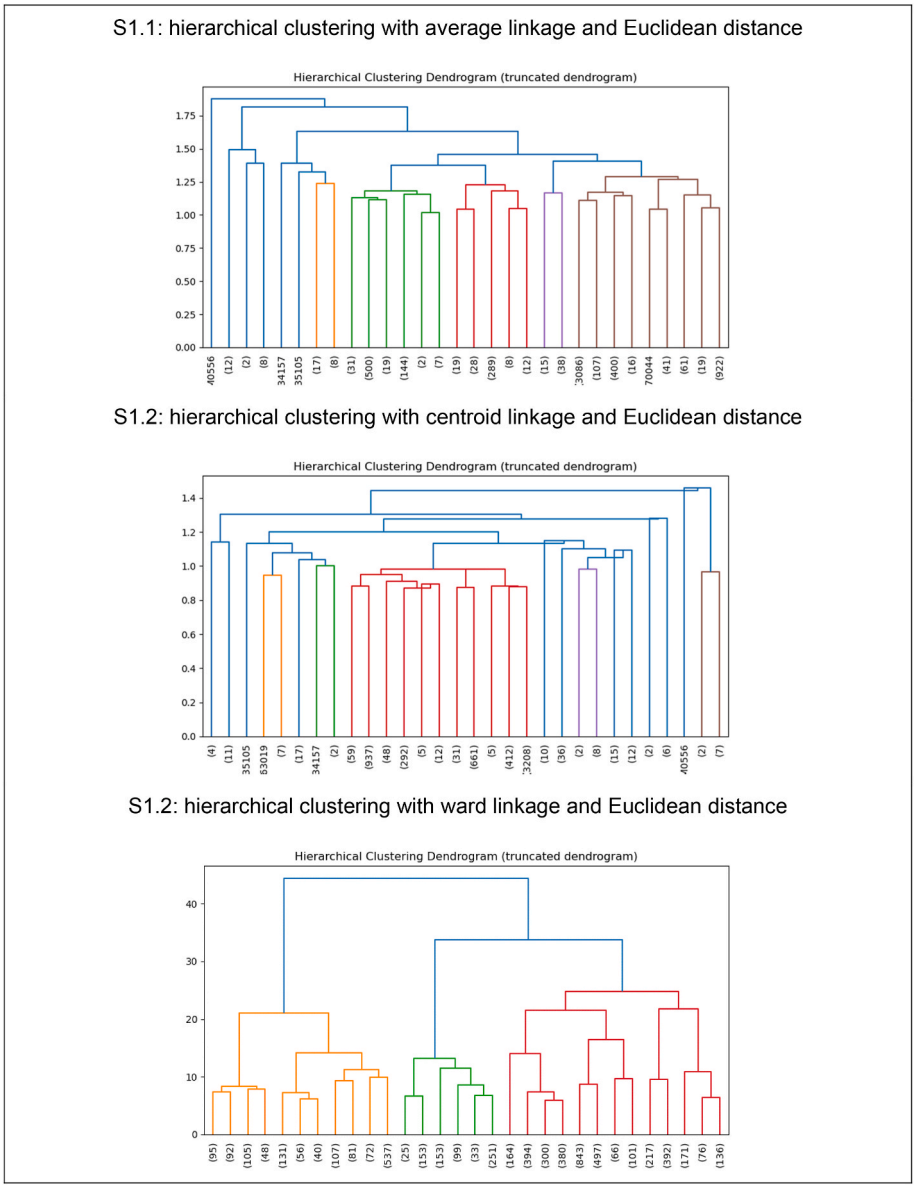

Fig. Annex 2. Dendrograms of the different hierarchical clusterings (S1).

Choosing for example four clusters leads to the following results (compare TableAnnex 5).

TableAnnex 5
Overview of results of different clusterings (S1).

Cluster	Total demand in GWh	Average demand in GWh	Number of DH areas	Petro-thermal	Hydro-thermal	WWTP	WtE	Industrial EH	Rivers and lakes	Biomass	Sludge	Highest potentials
S1.1: hierarchical clustering with average linkage and Euclidean distance												
1	115,084	84	1364	14%	26%	31%	6%	2%	99%	74%	1%	Rivers and lakes
2	31,584	44	714	24%	98%	34%	4%	5%	0%	72%	1%	Hydrothermal
3	2374	36	66	26%	33%	48%	5%	85%	100%	84%	1%	Rivers and lakes
4	583,086	159	3671	13%	1%	32%	4%	4%	1%	71%	1%	Biomass
S1.2: hierarchical clustering with centroid linkage and Euclidean distance												
1	1383	92	15	1%	30%	98%	85%	0%	100%	54%	2%	Rivers and lakes
2	730,605	126	5790	14%	19%	32%	4%	4%	25%	72%	1%	Biomass
3	77	9	9	98%	100%	19%	0%	92%	0%	69%	1%	Hydrothermal
4	64	64	1	1%	100%	14%	86%	100%	0%	3%	0%	Hydrothermal
S1.3: hierarchical clustering with ward linkage and Euclidean distance												
1	115,084	84	1364	14%	26%	31%	6%	2%	99%	74%	1%	Rivers and lakes
2	31,584	44	714	24%	98%	34%	4%	5%	0%	72%	1%	Hydrothermal
3	542,304	198	2745	4%	2%	18%	5%	6%	4%	70%	0%	Biomass
4	43,156	44	992	38%	1%	73%	0%	2%	0%	74%	1%	Biomass, WWTP
S1.4: k-means clustering												
1	103,854	93	1116	13%	3%	29%	6%	5%	98%	75%	1%	Rivers and lakes
2	506,273	193	2618	9%	1%	12%	4%	3%	1%	70%	0%	Biomass
3	59,652	59	1017	22%	1%	85%	5%	5%	0%	72%	1%	WWTP
4	62,350	59	1064	23%	98%	36%	5%	6%	32%	72%	1%	Hydrothermal

Comparing the output for five clusters shows that the clusterings lead to very different results. However, on a quantitative level, similarities can be observed: (i) There are several clusters where (at least) one source could cover (almost) all the demand. (ii) In all clusters, different renewable and waste heat sources can be used to cover the demand, i.e. all DH types represent multivalent networks.

B.2 Low-temperature scenario

As in the high-temperature scenario, we use the cophenetic correlation coefficient to compare different linkage types and dissimilarity calculations for hierarchical clusterings (TableAnnex 6).

TableAnnex 6
Cophenetic correlation coefficient for different hierarchical clusterings (S2).

metric	method					
	ward*	centroid*	single	complete	average	weighted
euclidean	**0.649**	0.747	0.571	0.733	**0.777**	0.668
cityblock (Manhattan distance)	–	–	0.522	0.654	**0.755**	0.687
mahalanobis	–	–	0.407	0.373	0.564	0.434
chebyshev	–	–	0.593	0.526	0.728	0.710

Note: Numbers in bold indicate which clustering methods are selected for further analysis. *Ward and centroid require Euclidean distance.

Again, we choose three hierarchical clusterings with a high cophenetic correlation coefficient and the k-means clustering for further analysis:

- S2.1: hierarchical clustering with average linkage and Euclidean distance,
- S2.2: hierarchical clustering with average linkage and Manhattan distance,
- S2.3: hierarchical clustering with ward linkage and Euclidean distance,
- S2.4: k-means clustering.

FigureAnnex 3 shows the dendrograms of the hierarchical clusterings.

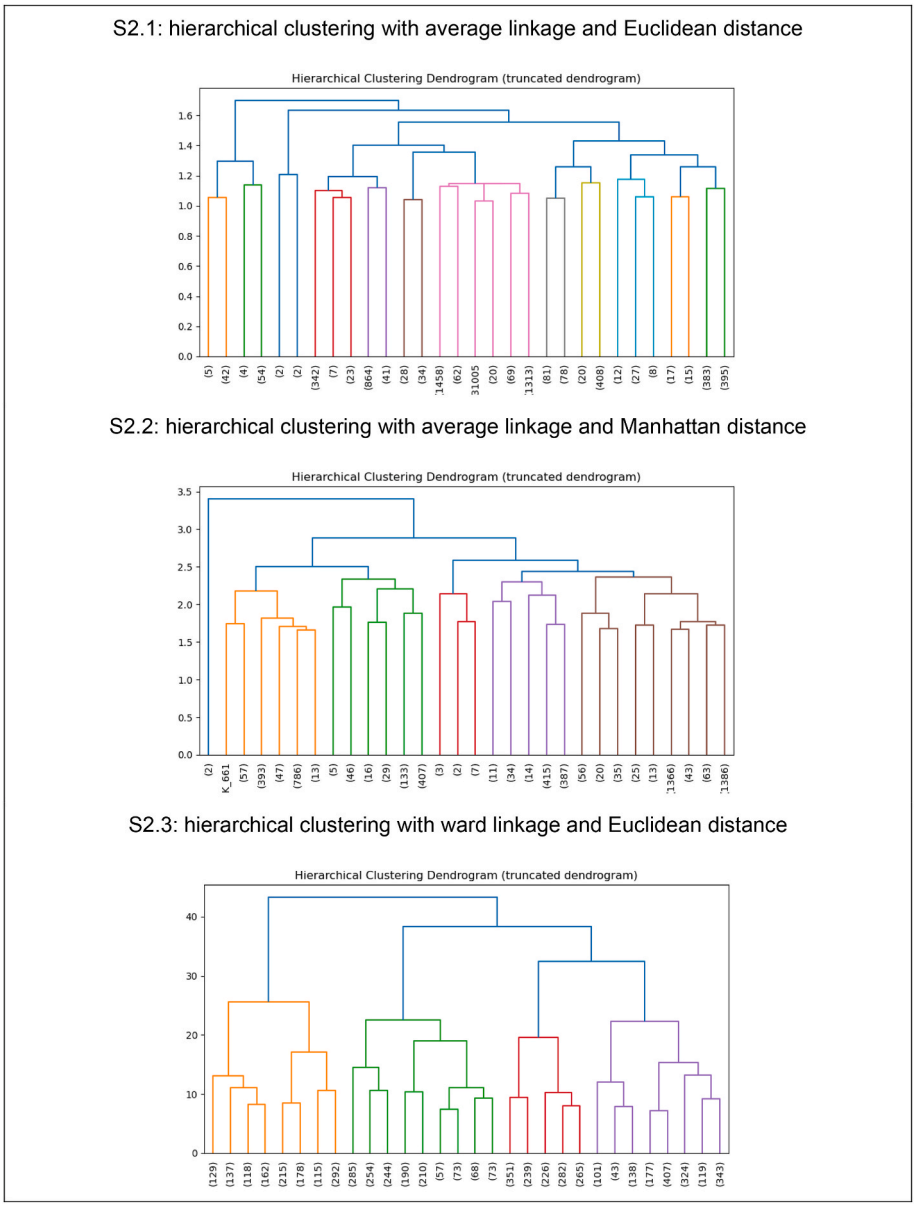

Fig. Annex 3. Dendrograms of the different hierarchical clusterings (S2).

Choosing again four clusters leads to the results shown in TableAnnex 7. As in the scenario with high temperatures, the clusterings lead to very different results. On a qualitative level, there is again the similarity that in several clusters (at least) one source could cover (almost) all of the demand and all types are multivalent networks.

TableAnnex 7
Overview of results of different clusterings (S2).

Cluster	Total demand in GWh	Average demand in GWh	Number of DH areas	Petro-thermal	Hydro-thermal	WWTP	WtE	Industrial EH	Rivers and lakes	Biomass	Sludge	Highest potential
S2.1: hierarchical clustering with average linkage and Euclidean distance												
1	177,87	169	105	12%	97%	38%	95%	1%	45%	66%	1%	Hydrothermal
2	728	182	4	5%	27%	13%	0%	91%	50%	10%	0%	Industrial EH
3	547,705	129	4262	49%	30%	37%	3%	5%	0%	73%	1%	Biomass
4	128,039	89	1444	43%	41%	36%	4%	7%	99%	77%	1%	Rivers and lakes
S2.2: hierarchical clustering with average linkage and Manhattan distance												
1	227	114	2	10%	0%	26%	0%	91%	100%	18%	1%	Rivers and lakes
2	133,527	69	1933	31%	99%	39%	6%	6%	33%	72%	1%	Hydrothermal

(*continued on next page*)

TableAnnex 7 (*continued*)

Cluster	Total demand in GWh	Average demand in GWh	Number of DH areas	Petro-thermal	Hydro-thermal	WWTP	WtE	Industrial EH	Rivers and lakes	Biomass	Sludge	Highest potential
3	6394	533	12	9%	21%	35%	56%	29%	25%	88%	1%	Biomass
4	554,112	143	3868	54%	2%	36%	5%	5%	22%	74%	1%	Biomass
S2.3: hierarchical clustering with ward linkage and Euclidean distance												
1	130,986	97	1346	40%	41%	35%	1%	3%	98%	77%	1%	Rivers and lakes
2	86,628	60	1454	38%	88%	38%	1%	16%	5%	74%	1%	Hydrothermal
3	42,118	31	1363	98%	1%	44%	0%	1%	0%	78%	1%	Petrothermal
4	434,528	263	1652	17%	8%	31%	16%	1%	6%	67%	1%	Biomass
S2.4: k-means clustering												
1	61,396	39	1590	96%	1%	45%	4%	5%	1%	79%	1%	Hydrothermal
2	87,501	66	1321	32%	99%	38%	5%	6%	1%	73%	1%	Petrothermal
3	133,172	91	1470	41%	43%	35%	7%	7%	99%	76%	1%	Rivers and lakes
4	412,191	287	1434	11%	2%	28%	5%	4%	1%	65%	1%	Biomass

Looking at both scenarios, the clusterings with average linkage type lead to groupings with only a few DH areas; i.e. only two or four areas in one cluster. These results are not in line with our objective to find representative DH types. In contrast, the clustering with ward linkage and the k-means clustering lead to a more equal distribution of areas into clusters. They also show several similarities, cross-validating the results. For example, in the low-temperature scenario (compare TableAnnex 7), both algorithms lead to (ii) one cluster with high average coverage of petrothermal, (ii) one cluster with high average coverage of hydrothermal, (iii) one cluster with high average coverage of rivers and lakes and (iv) one cluster with overall lower potentials, where only biomass can cover a larger share of the demand. Against this background, it seems reasonable to choose one of these clusterings for the analysis in this paper. For hierarchical clustering, it is not necessary to pre-specify the number of clusters. Because of this advantage, we decide to use hierarchical clustering with ward linkage and Euclidian distance and conduct further analyses to find a suitable number of clusters.

To decide on a reasonable number of clusters, we calculate the Silhouette score[8] and the Calinski-Harabasz score[9] for four, five and six clusters (compare TableAnnex 8). The silhouette coefficient measures how well an observation is clustered and it estimates the average distance between clusters. The best value is one and the worst value is minus one. The Calinski-Harabasz score is a variance ratio measurement, which measures the ratio between within-cluster dispersion and between-cluster dispersion. A higher Calinski-Harabasz score relates to a model with better-defined clusters.

TableAnnex 8
Silhouette and Calinski-Harabasz score.

Scenario	High temperatures		Low temperatures	
	Silhouette score	Calinski-Harabasz score	Silhouette score	Calinski-Harabasz score
4 clusters	0.285	**1468**	0.223	**1278**
5 clusters	0.276	1373	0.256	1223
6 clusters	**0.290**	1363	**0.273**	1175

Note: Numbers in bold indicate high values.

The comparison of the Silhouette score and the Calinski-Harabasz score shows that four clusters seem suitable as it reaches (rather) high values in both scenarios. Against this background, we choose to use hierarchical clustering with ward linkage and Euclidian distance with four clusters.

The following box shows the formulas for the Euclidean distance and the wards minimum variance.[10]

The Euclidean distance between the two figures $p = (p_1, ..., p_n)$ and $q = (q_1, ..., q_n)$ is calculated as follows:

$$d(p,q) = \sqrt{\sum_{i=1}^{n} (q_i - p_i)^2}.$$

The wards minimum variance is computed as follows:

$$d(u,v) = \sqrt{\frac{|v| + |s|}{T} \cdot d(v,s)^2 + \frac{|v| + |t|}{T} \cdot d(v,s)^2 - \frac{|v|}{T} \cdot d(v,s)^2}.$$

Thereby, u is the newly joined cluster consisting of the clusters s and t. The value v is an unused cluster and $T = |v| + |s| + |t|$. The operator $||$ calculates the cardinality of its argument.

[8] Based on the package SciKit; https://scikit-learn.org/stable/modules/generated/sklearn.metrics.silhouette_score.html.
[9] Based on the package SciKit; https://scikit-learn.org/stable/modules/generated/sklearn.metrics.calinski_harabasz_score.html.
[10] Compare https://docs.scipy.org/doc/scipy/reference/generated/scipy.spatial.distance.pdist.html#scipy.spatial.distance.pdist and https://docs.scipy.org/doc/scipy/reference/generated/scipy.cluster.hierarchy.linkage.html# scipy.cluster.hierarchy.linkage.

Appendix C. Country-specific results (output of clustering)

In the following tables, the results of the clustering for the DH types are listed. The average potentials per country and cluster can be calculated by dividing the sum of the respective potentials by the number of DH areas, i.e. sum potential = average potential * number of DH areas. The numbers are also published in the data repository as supplementary material to this publication [101].

C.1 High-temperature scenario

TableAnnex 9
Country-specific annual DH demand, number of DH areas and annual renewable and excess heat potentials per DH type.

Country	DH Type	Total DH demand in GWh	Average DH Demand in GWh	Number of DH areas	Sum of potentials in GWh							
					Petrothermal	Hydrothermal	WWTP	WtE	Industrial EH	Rivers and lakes	Biomass	Sludge
AT	1	4888	41	119	186	1090	1397	1432	134	4054	4536	141
	2	371	20	19	123	371	114	0	3	0	371	11
	3	12712	122	104	34	429	3697	2388	360	2255	4215	385
	4	482	16	30	50	3	433	0	2	0	471	35
BE	1	534	44	12	0	2	160	324	19	534	513	10
	2	33	17	2	0	28	17	7	0	0	22	1
	3	8050	278	29	1	169	1564	1859	1183	323	1434	142
	4	26	9	3	11	0	26	0	2	0	18	2
BG	1	202	101	2	0	0	47	0	0	202	202	0
	2	60	30	2	6	60	0	0	12	0	60	0
	3	5885	218	27	1	19	1372	0	186	13	3953	0
	4	275	92	3	0	0	228	0	0	0	275	0
CZ	1	2085	39	53	297	297	693	0	15	2029	1675	15
	2	397	79	5	5	381	65	0	1	0	235	2
	3	25228	138	183	308	444	4919	869	395	2447	15305	119
	4	1053	24	43	217	0	761	0	1	0	1019	16
DE	1	37655	97	389	1886	9285	12208	8433	1364	35803	16778	402
	2	8351	39	216	810	8012	3211	1230	151	0	6801	118
	3	95391	283	337	3129	6617	22691	23481	1953	10579	37572	873
	4	7547	26	286	4051	211	5227	9	224	0	5253	170
DK	2	137	46	3	37	137	72	10	0	0	97	1
	3	19588	306	64	71	482	3846	2252	24	0	5407	62
	4	1455	104	14	63	2	971	130	17	0	731	9
EE	1	237	47	5	0	0	91	0	0	237	237	0
	3	3531	82	43	0	0	535	0	20	440	3531	0
	4	216	43	5	0	0	213	0	0	0	216	0
EL	1	147	73	2	0	0	0	0	0	106	45	1
	3	8729	178	49	13	0	980	0	197	0	3661	114
	4	529	38	14	226	0	295	0	1	60	516	9
ES	1	1352	38	36	80	0	444	0	8	1351	1044	5
	3	29559	120	246	472	0	9923	1520	991	523	15113	138
	4	13190	118	112	383	0	10520	355	136	0	9495	100
FI	1	10745	160	67	0	0	13	42	494	10745	10745	1
	3	24181	255	95	0	0	0	264	359	1060	15135	0
FR	1	8547	52	163	844	5969	2211	2523	148	7686	6065	0
	2	7125	40	180	1442	6556	1975	914	216	180	6123	0
	3	88255	446	198	1713	6531	19042	14025	1328	3478	31804	1
	4	3416	31	110	2012	63	1865	83	50	220	2922	0
HR	1	2092	523	4	79	2086	684	0	16	1381	1158	6
	2	30	30	1	0	30	20	0	30	0	17	0
	3	942	118	8	7	14	219	0	28	14	885	2
	4	290	290	1	0	0	290	0	21	0	274	2
HU	1	1834	71	26	258	1666	691	0	32	1590	1660	11
	2	3625	95	38	975	3559	1706	8	33	60	3552	25
	3	11276	3759	3	210	3146	2233	457	180	900	3329	27
	4	229	76	3	154	0	187	0	0	0	229	2
IE	1	209	23	9	0	0	30	0	0	209	209	0
	3	1101	36	31	0	0	428	469	110	0	1101	0
	4	13	7	2	0	0	10	0	0	0	13	0
IT	1	6369	42	153	4	446	2163	1152	134	6203	3530	4
	2	5384	40	133	479	5225	1638	295	293	0	3324	4
	3	73129	115	636	311	5707	17543	5616	1548	2199	32289	38
	4	4414	29	152	144	123	3921	14	63	0	2486	7
LT	1	1686	130	13	53	0	510	0	15	1686	1686	0
	3	4885	136	36	28	0	1087	0	43	1660	4885	0
	4	346	43	8	56	0	255	0	0	0	346	0
LU	1	94	13	7	0	0	1	0	0	94	9	0
	3	2683	60	45	0	20	280	195	52	0	245	0
	4	82	20	4	0	0	82	0	0	0	7	0
LV	1	3569	99	36	0	0	886	0	0	3414	3569	0
	3	1233	39	32	0	0	226	0	10	120	1233	0

(*continued on next page*)

TableAnnex 9 (*continued*)

Country	DH Type	Total DH demand in GWh	Average DH Demand in GWh	Number of DH areas	Sum of potentials in GWh							
					Petrothermal	Hydrothermal	WWTP	WtE	Industrial EH	Rivers and lakes	Biomass	Sludge
	4	73	12	6	0	0	58	0	0	0	73	0
NL	1	2042	79	26	151	1372	800	390	59	2042	1061	7
	2	3357	45	75	502	3316	963	1131	122	0	1577	12
	3	17954	321	56	359	848	3432	8848	651	100	660	40
	4	1324	74	18	204	93	1125	0	0	0	643	8
PL	1	7969	97	82	604	971	2401	0	98	7713	7561	39
	2	806	50	16	144	747	316	0	3	60	806	4
	3	46426	179	259	531	127	10396	16	661	5408	37701	173
	4	4137	37	112	913	12	3005	0	38	0	3521	37
PT	1	150	19	8	52	0	106	0	4	150	102	3
	3	2900	223	13	139	0	1294	636	133	48	543	39
	4	515	57	9	51	0	486	0	3	0	246	11
RO	1	1669	64	26	55	428	855	0	33	1589	1656	1
	2	24	24	1	2	16	0	0	0	0	24	0
	3	8277	176	47	0	0	2333	0	350	386	5532	3
	4	2483	89	28	4	334	2040	0	21	0	2483	2
SE	1	19318	217	89	829	0	2339	1672	426	17376	13494	205
	3	45919	285	161	534	0	3846	5052	636	1573	21971	382
	4	523	40	13	248	0	224	0	27	0	338	19
SI	1	370	46	8	9	218	95	0	11	356	234	2
	3	1249	89	14	11	11	54	12	33	203	228	7
	4	59	20	3	0	0	59	0	0	0	0	1
SK	1	1322	46	29	148	313	520	0	52	1288	1188	0
	2	1883	82	23	435	1804	507	0	38	60	1826	0
	3	3221	111	29	67	286	1432	47	190	843	1730	0
	4	478	37	13	84	40	300	0	0	0	470	0

C.2 Low-temperature scenario

TableAnnex 10
Country-specific annual DH demand, number of DH areas and annual renewable and excess heat potentials per DH type.

Country	DH type	Total DH demand in GWh	Average DH demand in GWh	Number of DH areas	Sum of potentials in GWh							
					Petrothermal	Hydrothermal	WWTP	WtE	Industrial EH	Rivers and lakes	Biomass	Sludge
AT	1	3341	30	111	797	386	1616	68	138	3274	2963	152
	2	1914	50	38	501	1727	302	0	364	523	1914	32
	3	488	12	42	478	0	139	0	0	0	488	13
	4	11755	145	81	673	1002	4531	4040	416	3351	3836	404
BE	1	101	14	7	63	0	22	0	0	101	84	5
	2	1618	116	14	155	1140	444	772	826	289	835	34
	3	31	8	4	31	2	25	0	3	0	24	2
	4	6447	307	21	135	4	1634	1637	1005	541	1010	122
BG	1	192	96	2	23	192	57	0	0	192	192	0
	2	2433	90	27	668	2205	628	0	323	12	2378	0
	4	3465	693	5	24	857	1303	0	17	0	1819	0
CZ	1	2941	49	60	1714	1338	1180	0	6	2639	2619	25
	2	2943	75	39	930	2576	770	0	629	324	2337	18
	3	3181	24	134	3081	11	1587	0	8	0	3095	33
	4	18211	357	51	2510	334	4169	956	286	2231	9728	84
DE	1	44232	121	366	4841	19657	15535	10684	2570	38198	16463	447
	2	17325	51	338	2616	15185	6102	1771	2483	2384	14568	227
	3	7394	22	329	7070	67	4262	0	203	0	5000	153
	4	72290	371	195	8924	16102	24463	23633	1682	8581	29391	814
DK	2	6770	130	52	703	6751	2712	797	71	0	3387	35
	3	807	81	10	745	70	430	35	0	0	456	6
	4	12507	658	19	441	2400	2700	1774	0	0	2516	35
EE	1	913	130	7	0	0	268	0	0	816	913	0
	2	46	15	3	0	0	15	0	27	0	46	0
	4	2819	66	43	0	0	685	0	17	0	2819	0
EL	1	258	86	3	151	0	0	0	1	205	164	3
	2	79	26	3	17	0	5	0	55	0	73	2
	3	424	28	15	412	0	236	0	3	0	369	6
	4	8157	185	44	218	0	1291	0	218	0	3469	119
ES	1	1855	46	40	1371	0	466	12	13	1601	1529	6
	2	901	38	24	496	0	246	0	739	31	686	6
	3	5817	30	195	5427	0	2919	0	202	0	4948	35
	4	33247	246	135	4400	0	20015	1950	832	323	18102	209
FI	1	12328	174	71	0	0	16	38	961	11310	12328	1

(*continued on next page*)

TableAnnex 10 (*continued*)

Country	DH type	Total DH demand in GWh	Average DH demand in GWh	Number of DH areas	Sum of potentials in GWh							
					Petrothermal	Hydrothermal	WWTP	WtE	Industrial EH	Rivers and lakes	Biomass	Sludge
	2	221	74	3	0	0	0	0	109	0	221	0
	4	20570	234	88	0	0	0	298	381	303	12163	0
FR	1	11021	74	148	2449	6980	4369	1801	1423	8471	9627	0
	2	13493	56	241	3780	11115	4100	2181	755	512	11811	0
	3	4922	38	128	4696	17	2263	563	92	81	4406	0
	4	72355	540	134	4072	18295	19166	14734	1666	3856	19923	1
HR	1	1981	495	4	180	1976	835	0	30	1842	1180	6
	2	45	22	2	0	45	24	0	40	16	27	0
	4	1155	144	8	0	0	543	0	55	0	1155	4
HU	1	1709	68	25	341	1550	723	0	44	1551	1570	11
	2	3505	88	40	1316	3486	2021	9	80	110	3418	27
	3	203	51	4	203	0	179	0	0	0	196	2
	4	10670	10670	1	480	5662	2726	503	304	1210	3378	29
IE	1	198	22	9	0	0	31	0	0	198	198	0
	2	256	37	7	10	142	9	77	131	0	256	0
	4	801	31	26	0	11	416	379	0	0	801	0
IT	1	5774	40	144	391	4059	2305	604	209	5388	3566	4
	2	21310	56	380	2856	19548	7361	628	1816	1343	10519	14
	3	2257	18	122	1922	93	916	8	80	0	1317	2
	4	55336	129	428	2114	5800	19202	6515	1413	2229	26328	35
LT	1	3835	256	15	90	0	1164	0	33	3821	3835	0
	2	130	130	1	10	0	42	0	64	0	130	0
	3	634	37	17	625	0	213	0	0	0	634	0
	4	1960	82	24	358	0	803	0	7	0	1960	0
LU	1	89	13	7	83	0	2	0	0	89	9	0
	2	216	31	7	61	113	0	0	68	0	21	0
	3	120	9	13	116	0	9	0	0	0	12	0
	4	2286	79	29	219	208	410	215	41	0	224	0
LV	1	3628	95	38	203	0	1209	0	0	3546	3628	0
	2	43	22	2	0	0	17	0	23	0	43	0
	3	56	19	3	52	0	18	0	0	0	56	0
	4	896	29	31	20	0	178	0	1	0	896	0
NL	1	1366	62	22	289	1276	573	0	35	1366	814	5
	2	4647	46	100	1288	4069	2050	38	1098	240	1712	18
	3	351	25	14	321	4	207	0	0	0	213	1
	4	17036	437	39	1114	3732	4517	10737	668	425	1243	46
PL	1	11657	124	94	5032	2203	4040	0	781	10780	11279	67
	2	4085	64	64	1711	3316	1600	0	501	471	3878	20
	3	7411	37	199	7132	145	3383	0	84	0	6943	47
	4	33116	296	112	4171	584	10111	18	394	3454	25905	132
PT	1	135	17	8	101	0	83	0	35	135	96	3
	2	175	35	5	175	0	103	0	125	30	70	3
	3	257	26	10	253	0	172	0	8	0	177	5
	4	2814	402	7	396	0	1794	695	15	24	534	45
RO	1	2180	75	29	1434	722	1169	0	162	1807	2168	1
	2	1001	111	9	277	710	425	0	295	82	993	0
	3	1816	42	43	1773	0	1166	0	21	0	1816	1
	4	6812	324	21	777	1143	2985	0	298	161	4331	3
SE	1	18935	204	93	5263	0	2956	1403	880	17959	14236	232
	2	787	79	10	648	0	101	10	426	135	510	9
	3	5680	84	68	4848	0	693	90	61	81	3435	62
	4	36957	402	92	4584	0	3938	5749	525	1911	17351	334
SI	1	444	40	11	130	294	121	13	28	444	309	4
	2	105	35	3	23	77	0	0	17	6	77	0
	3	23	23	1	23	0	0	0	1	0	23	0
	4	1019	102	10	2	4	106	0	20	161	29	6
SK	1	1875	59	32	736	993	869	0	147	1663	1749	0
	2	2578	61	42	1047	2509	1003	0	132	148	2474	0
	3	246	21	12	242	18	96	0	1	0	238	0
	4	1848	231	8	128	932	1313	52	159	605	500	0

References

[1] D. Connolly, H. Lund, B.V. Mathiesen, et al., Heat Roadmap Europe: combining district heating with heat savings to decarbonise the EU energy system, Energy Pol. 65 (2014) 475–489, https://doi.org/10.1016/j.enpol.2013.10.035.

[2] L. Kranzl, S. Forthuber, M. Fallahnejad, et al., ENER/C1/2018-494 - Renewable Space Heating under the Revised Renewable Energy Directive: Final Report, 2022. Luxembourg.

[3] P. Manz, T. Fleiter, S. Alibas, et al., Finding an Optimal District Heating Market Share in 2050 for EU-27: Comparison of Modelling Approaches, 2022 eceee 2022 Summer Study.

[4] Publications Office, Directive (EU) 2018/844 of the European Parliament and of the Council of 30 May 2018 Amending Directive 2010/31/EU on the Energy Performance of Buildings and Directive 2012/27/EU on Energy Efficiency, revised in 2023, 2023.

[5] U. Persson, E. Wiechers, B. Möller, et al., Heat Roadmap Europe: heat distribution costs, Energy 176 (2019) 604–622, https://doi.org/10.1016/j.energy.2019.03.189.

[6] U. Persson, S. Werner, Heat distribution and the future competitiveness of district heating, Appl. Energy 88 (2011) 568–576, https://doi.org/10.1016/j.apenergy.2010.09.020.

[7] M. Fallahnejad, L. Kranzl, M. Hummel, District heating distribution grid costs: a comparison of two approaches, IJSEPM 34 (2022) 79–90, https://doi.org/10.54337/ijsepm.7013.

[8] M. Fallahnejad, M. Hartner, L. Kranzl, et al., Impact of distribution and transmission investment costs of district heating systems on district heating potential, Energy Proc. 149 (2018) 141–150, https://doi.org/10.1016/j.egypro.2018.08.178.

[9] M. Hummel, A. Müller, M. Fallahnejad, et al., The economic value of existing district heating grid infrastructure for the transition towards a carbon neutral heating system. Internationale Energiewirtschaftstagung an der TU Wien (IEWT) 12, 2021.

[10] L. Sánchez-García, H. Averfalk, E. Möllerström, et al., Understanding effective width for district heating, Energy 277 (2023) 127427, https://doi.org/10.1016/j.energy.2023.127427.

[11] Leurent M Analysis of the district heating potential in French regions using a geographic information system, Appl. Energy (2019), https://doi.org/10.1016/j.apenergy.2019.113460.

[12] European Commission, District Heating and Cooling in the European Union: Overview of District Heating and Cooling Markets and Regulatory Frameworks under the Revised Renewable Energy Directive, 2022.

[13] Eurostat, Production of Electricity and Derived Heat by Type of Fuel (Nrg_bal_peh), 2023.

[14] S. Boesten, W. Ivens, S.C. Dekker, et al., 5th generation district heating and cooling systems as a solution for renewable urban thermal energy supply, Adv. Geosci. 49 (2019) 129–136, https://doi.org/10.5194/adgeo-49-129-2019.

[15] S. Buffa, M. Cozzini, M. D'Antoni, et al., 5th generation district heating and cooling systems: a review of existing cases in Europe, Renew. Sustain. Energy Rev. 104 (2019) 504–522, https://doi.org/10.1016/j.rser.2018.12.059.

[16] H. Lund, P.A. Østergaard, T.B. Nielsen, et al., Perspectives on fourth and fifth generation district heating, Energy 227 (2021) 120520, https://doi.org/10.1016/j.energy.2021.120520.

[17] A. Volkova, I. Pakere, L. Murauskaite, et al., 5th generation district heating and cooling (5GDHC) implementation potential in urban areas with existing district heating systems, Energy Rep. 8 (2022) 10037–10047, https://doi.org/10.1016/j.egyr.2022.07.162.

[18] H. Lund, S. Werner, R. Wiltshire, et al., 4th generation district heating (4GDH), Energy 68 (2014) 1–11, https://doi.org/10.1016/j.energy.2014.02.089.

[19] A.M. Jodeiri, M.J. Goldsworthy, S. Buffa, et al., Role of sustainable heat sources in transition towards fourth generation district heating – a review, Renew. Sustain. Energy Rev. 158 (2022) 112156, https://doi.org/10.1016/j.rser.2022.112156.

[20] H. Averfalk, et al., Kristina Lygnerud and Sven Werner (2021) Low-Temperature District Heating Implementation Guidebook, IEA DHC Report, 2021.

[21] Pompei L, Nardecchia F, Mattoni B et al. Combining the exergy and energy analysis for the assessment of district heating powered by renewable sources. Conference Proceedings 2019 IEEE International Conference on Environment and Electrical Engineering and 2019 IEEE Industrial and Commercial Power Systems Europe (EEEIC/I & CPS Europe). IEEE, Piscataway, NJ..

[22] N. Nord, D. Schmidt, A.M.D. Kallert, Necessary measures to include more distributed renewable energy sources into district heating system, Energy Proc. 116 (2017) 48–57, https://doi.org/10.1016/j.egypro.2017.05.054.

[23] M. Rämä, M. Wahlroos, Introduction of new decentralised renewable heat supply in an existing district heating system, Energy 154 (2018) 68–79, https://doi.org/10.1016/j.energy.2018.03.105.

[24] R. Geyer, J. Krail, B. Leitner, et al., Energy-economic assessment of reduced district heating system temperatures, Smart Energy 2 (2021) 100011, https://doi.org/10.1016/j.segy.2021.100011.

[25] N. Bertelsen, B.V. Mathiesen, S.R. Djørup, et al., Integrating Low-Temperature Renewables in District Energy Systems: Guidelines for Policy Makers, International Renewable Energy Agency, 2021.

[26] I. Sarbu, M. Mirza, D. Muntean, Integration of renewable energy sources into low-temperature district heating systems: a review, Energies 15 (2022) 6523, https://doi.org/10.3390/en15186523.

[27] H. Lund, N. Duic, P.A. Østergaard, et al., Future district heating systems and technologies: on the role of smart energy systems and 4th generation district heating, Energy 165 (2018) 614–619, https://doi.org/10.1016/j.energy.2018.09.115.

[28] H. Lund, P.A. Østergaard, M. Chang, et al., The status of 4th generation district heating: research and results, Energy 164 (2018) 147–159, https://doi.org/10.1016/j.energy.2018.08.206.

[29] J.C. Santamarta, A. García-Gil, M.C. Del Expósito, et al., The clean energy transition of heating and cooling in touristic infrastructures using shallow geothermal energy in the Canary Islands, Renew. Energy 171 (2021) 505–515, https://doi.org/10.1016/j.renene.2021.02.105.

[30] A. Walch, N. Mohajeri, A. Gudmundsson, et al., Quantifying the technical geothermal potential from shallow borehole heat exchangers at regional scale, Renew. Energy 165 (2021) 369–380, https://doi.org/10.1016/j.renene.2020.11.019.

[31] C. Tissen, K. Menberg, S.A. Benz, et al., Identifying key locations for shallow geothermal use in Vienna, Renew. Energy 167 (2021) 1–19, https://doi.org/10.1016/j.renene.2020.11.024.

[32] A.S. Pratiwi, E. Trutnevyte, Decision paths to reduce costs and increase economic impact of geothermal district heating in Geneva, Switzerland, Appl. Energy 322 (2022) 119431, https://doi.org/10.1016/j.apenergy.2022.119431.

[33] S. Kaur, J.S. Yadav, R. Bhambri, et al., Assessment of geothermal potential of Kumaun Himalaya: a perspective for harnessing green energy, Renew. Energy 212 (2023) 940–952, https://doi.org/10.1016/j.renene.2023.05.112.

[34] V.M. Soltero, R. Chacartegui, C. Ortiz, et al., Potential of biomass district heating systems in rural areas, Energy 156 (2018) 132–143, https://doi.org/10.1016/j.energy.2018.05.051.

[35] J. Idsø, T. Årethun, Water-thermal energy production system: a case study from Norway, Sustainability 9 (2017) 1665, https://doi.org/10.3390/su9091665.

[36] Y.-J. Baik, M. Kim, K.-C. Chang, et al., Potential to enhance performance of seawater-source heat pump by series operation, Renew. Energy 65 (2014) 236–244, https://doi.org/10.1016/j.renene.2013.09.021.

[37] Y. Jung, J. Kim, H. Kim, et al., Comprehensive feasibility investigation of river source heat pump systems in terms of life cycle, Appl. Therm. Eng. 188 (2021) 116655, https://doi.org/10.1016/j.applthermaleng.2021.116655.

[38] E. Mäki, L. Kannari, I. Hannula, et al., Decarbonization of a district heating system with a combination of solar heat and bioenergy: a techno-economic case study in the Northern European context, Renew. Energy 175 (2021) 1174–1199, https://doi.org/10.1016/j.renene.2021.04.116.

[39] A. Aliana, M. Chang, P.A. Østergaard, et al., Performance assessment of using various solar radiation data in modelling large-scale solar thermal systems integrated in district heating networks, Renew. Energy 190 (2022) 699–712, https://doi.org/10.1016/j.renene.2022.03.163.

[40] A. Dénarié, F. Fattori, G. Spirito, et al., Assessment of waste and renewable heat recovery in DH through GIS mapping: the national potential in Italy, Smart Energy 1 (2021) 100008, https://doi.org/10.1016/j.segy.2021.100008.

[41] P. Manz, M. Fallahnejad, A. Billerbeck, Potentials for district heating generation in a climate-neutral energy system, 12. Internationale Energiewirtschaftstagung an der TU Wien (IEWT), 2021.

[42] J. Pelda, F. Stelter, S. Holler, Potential of integrating industrial waste heat and solar thermal energy into district heating networks in Germany, Energy 203 (2020) 117812, https://doi.org/10.1016/j.energy.2020.117812.

[43] M. Jakob, U. Reiter, G. Catenazzi, et al., Erneuerbare- und CO2-freie Wärmeversorgung Schweiz: Eine Studie zur Evaluation von Erfordernissen und Auswirkungen, 2020.

[44] R. Bracke, E. Huenges, Roadmap Tiefe Geothermie für Deutschland: Handlungsempfehlungen für Politik, Wirtschaft und Wissenschaft für eine erfolgreiche Wärmewende. Strategiepapier von sechs Einrichtungen der Fraunhofer-Gesellschaft und der Helmholtz-Gesellschaft, Fraunhofer-Gesellschaft, 2021.

[45] J. Limberger, P. Calcagno, A. Manzella, et al., Assessing the prospective resource base for enhanced geothermal systems in Europe, Geoth. Energ. Sci. 2 (2014) 55–71, https://doi.org/10.5194/gtes-2-55-2014.

[46] F. Dalla Longa, L.P. Nogueira, J. Limberger, et al., Scenarios for geothermal energy deployment in Europe, Energy 206 (2020) 118060, https://doi.org/10.1016/j.energy.2020.118060.

[47] Büro für Technikfolgen-Abschätzung beim Deutschen Bundestag, Möglichkeiten Geothermischer Stromerzeugung in Deutschland: Sachstandsbericht, 2003.

[48] K. Könighofer, G. Domberger, S. Gunzy, et al., Potenzial der Tiefengeothermie für die Fernwärme- und Stromproduktion in Österreich: Endbericht GeoEnergie2050, 2014.

[49] S. Braungardt, K. Hennenberg, I. Ganal, et al., The Role of Biomass in the Decarbonisation of the Heating Sector, Study on behalf of the European, Climate Foundation (2022).

[50] Imperial College London, Sustainable Biomass Availability in the EU, to 2050: Ref: RED II Annex IX A/B, 2021.

[51] UK Department of Energy & Climate Change, National Heat Map: Water Source Heat Map Layer, 2015.

[52] A. Gaudard, M. Schmid, A. Wüest, Thermische Nutzung von Seen und Flüssen: Potenzial der Schweizer Oberflächengewässer, AQUA & GAS N°2, 26-33, 2018.

[53] V. Somogyi, V. Sebestyén, E. Domokos, Assessment of wastewater heat potential for district heating in Hungary, Energy 163 (2018) 712–721, https://doi.org/10.1016/j.energy.2018.07.157.

[54] K. Münch, S. Blömer, L. Lütkes, et al., Abwasserwärmenutzung aus dem Auslauf von Kläranlagen: Lokalisierung von Standorten in Baden-Württemberg, 2022.

[55] U. Persson, H. Averfalk, Accessible urban waste heat: deliverable D1.4 ReUseHeat, 2018.

[56] S. Nielsen, K. Hansen, R. Lund, et al., Unconventional excess heat sources for district heating in a national energy system context, Energies 13 (2020) 5068, https://doi.org/10.3390/en13195068.

[57] P. Manz, T. Fleiter, W. Eichhammer, The effect of low-carbon processes on industrial excess heat potentials for district heating in the EU: a GIS-based analysis, Smart Energy 10 (2023) 100103, https://doi.org/10.1016/j.segy.2023.100103.

[58] U. Persson, B. Möller, S. Werner, Heat Roadmap Europe: identifying strategic heat synergy regions, Energy Pol. 74 (2014) 663–681, https://doi.org/10.1016/j.enpol.2014.07.015.

[59] M. Papapetrou, G. Kosmadakis, A. Cipollina, et al., Industrial waste heat: estimation of the technically available resource in the EU per industrial sector, temperature level and country, Appl. Therm. Eng. 138 (2018) 207–216, https://doi.org/10.1016/j.applthermaleng.2018.04.043.

[60] G. Bianchi, G.P. Panayiotou, L. Aresti, et al., Estimating the waste heat recovery in the European Union Industry, Energ Ecol. Environ. 4 (2019) 211–221, https://doi.org/10.1007/s40974-019-00132-7.

[61] S. Stark, F. Uthoff, J.A. Miller, Leitfaden zur Erschließung von Abwärmequellen für die Fernwärmeversorgung: Ein Leitfaden des AGFW, 2020.

[62] U. Persson, M. Münster, Current and future prospects for heat recovery from waste in European district heating systems: a literature and data review, Energy 110 (2016) 116–128, https://doi.org/10.1016/j.energy.2015.12.074.
[63] K. Weber, P. Quicker, J. Hanewinkel, et al., Status of waste-to-energy in Germany, Part I - waste treatment facilities, Waste Manag. Res. 38 (2020) 23–44, https://doi.org/10.1177/0734242X19894632.
[64] Europa-Universität Flensburg, Halmstad University, Aalborg University, Pan-European Thermal Atlas 5.1 (PETA 5.1), sEEnergies, 2021.
[65] HotMaps, Hotmaps Toolbox: the Open Source Mapping and Planning Tool for Heating and Cooling. EU Horizon 2020 Research and Innovation Program under Grant Agreement No. 723677. 2016-2020, 2016 - 2020.
[66] D. Moreno, S. Nielsen, U. Persson, The European Waste Heat Map: ReUseHeat Project, 2022.
[67] U. Persson, B. Möller, E. Wiechers, Methodologies and Assumptions Used in the Mapping: Deliverable 2.3: A Final Report Outlining the Methodology and Assumptions Used in the Mapping. Heat Roadmap Europe 2050, A Low-Carbon Heating and Cooling Strategy, 2017.
[68] U. Persson, B. Möller, L.S. García, et al., District Heating Investment Costs and Allocation of Local Resources for EU28 in 2030 and 2050: Deliverable 4.5 sEEnergies - Quantification of Synergies between Energy Efficiency First Principle and Renewable Energy Systems, 2021.
[69] B. Möller, E. Wiechers, L. Sánchez-García, et al., Spatial Models and Spatial Analytics Results: Deliverable 5.7 sEEnergies - Quantification of Synergies between Energy Efficiency First Principle and Renewable Energy Systems, 2022.
[70] G. Spirito, A. Dénarié, F. Fattori, et al., Potential diffusion of renewables-based DH assessment through clustering and mapping: a case study in milano, Energies 14 (2021) 2627, https://doi.org/10.3390/en14092627.
[71] P. Manz, K. Kermeli, U. Persson, et al., Decarbonizing district heating in EU-27 + UK: how much excess heat is available from industrial sites? Sustainability 13 (2021) 1439, https://doi.org/10.3390/su13031439.
[72] F. Bühler, S. Petrović, F.M. Holm, et al., Spatiotemporal and economic analysis of industrial excess heat as a resource for district heating, Energy 151 (2018) 715–728, https://doi.org/10.1016/j.energy.2018.03.059.
[73] J. Unternährer, S. Moret, S. Joost, et al., Spatial clustering for district heating integration in urban energy systems: application to geothermal energy, Appl. Energy 190 (2017) 749–763, https://doi.org/10.1016/j.apenergy.2016.12.136.
[74] X. Li, A. Walch, S. Yilmaz, et al., Optimal spatial resource allocation in networks: application to district heating and cooling, Comput. Ind. Eng. 171 (2022) 108448, https://doi.org/10.1016/j.cie.2022.108448.
[75] C. Scaramuzzino, G. Garegnani, P. Zambelli, Integrated approach for the identification of spatial patterns related to renewable energy potential in European territories, Renew. Sustain. Energy Rev. 101 (2019) 1–13, https://doi.org/10.1016/j.rser.2018.10.024.
[76] J.F. Marquant, L.A. Bollinger, R. Evins, et al., A new combined clustering method to Analyse the potential of district heating networks at large-scale, Energy 156 (2018) 73–83, https://doi.org/10.1016/j.energy.2018.05.027.
[77] M.S. Triebs, E. Papadis, H. Cramer, et al., Landscape of district heating systems in Germany – status quo and categorization, Energy Convers. Manag. X 9 (2021) 100068, https://doi.org/10.1016/j.ecmx.2020.100068.
[78] European Commission, Directorate-General for Energy, S. Braungardt, V. Bürger, T. Fleiter, et al., Renewable heating and cooling pathways – Towards full decarbonisation by 2050 – Final report, Publications Office of the European Union, 2023, https://data.europa.eu/doi/10.2833/036342.
[79] P. Sorknæs, P.A. Østergaard, J.Z. Thellufsen, et al., The benefits of 4th generation district heating in a 100% renewable energy system, Energy 213 (2020) 119030, https://doi.org/10.1016/j.energy.2020.119030.
[80] P. Ruiz, ENSPRESO - BIOMASS, European Commission, Joint Research Centre (JRC), 2019. http://data.europa.eu/89h/74ed5a04-7d74-4807-9eab-b94774309d9f. (Accessed 15 January 2023).
[81] European Commission, Atlas of Geothermal Resources in Europe, 2002.
[82] GeoDH European Geothermal Energy Council, GeoDH Geographical Information System (Map), 2014.
[83] Copernicus Climate Change Service (C3S) Climate Data Store (CDS) (2021): Hydrology-related climate impact indicators from 1970 to 2100 derived from bias adjusted European climate projections. https://doi.org/10.24381/cds.73237ad6. (Accessed 19 August 2022).
[84] P. Ruiz, W. Nijs, D. Tarvydas, et al., ENSPRESO - an open, EU-28 wide, transparent and coherent database of wind, solar and biomass energy potentials, Energy Strategy Rev. 26 (2019) 100379, https://doi.org/10.1016/j.esr.2019.100379.
[85] European Geothermal Energy Council, 2020 EGEC Geothermal Market Report: Key Findings, 2021.
[86] GeoDH European Geothermal Energy Council, Developing Geothermal District Heating in Europe, 2014.
[87] Umweltbundesamt, Kommunaler Klimaschutz durch Verbesserung der Effizienz in der Fernwärmeversorgung mittels Nutzung von Niedertemperaturwärmequellen am Beispiel tiefengeothermischer Ressourcen: Abschlussbericht, 2020.
[88] G. Yu, H. Li, C. Liu, et al., Thermal and hydraulic characteristics of a new proposed flyover-crossing fracture configuration for the enhanced geothermal system, Renew. Energy 211 (2023) 859–873, https://doi.org/10.1016/j.renene.2023.04.148.
[89] European Commission, Potential Impacts of Solar, Geothermal and Ocean Energy on Habitats and Species Protected under the Birds and Habitats Directives: Final Report, 2020.
[90] R. Schulz, E. Suchi, J. Dittmann, et al., Geothermie-Atlas zur Darstellung möglicher Nutzungskonkurrenzen zwischen CCS und Tiefer Geothermie: Endbericht, 2013.
[91] M. Douziech, I. Blanc, L. Damen, et al., Generation of Simplified Parametrised Models for a Selection of GEOENVI Geothermal Installations Categories: GEONEVI Deliverable D3.4, 2020.
[92] V. Wilk, B. Windholz, M. Hartl, et al., Techno-ökonomische Analyse der Integration von flusswassergespeisten Großwärmepumpen in FW-Netzen, 2015.
[93] Gewässerkundlicher Dienst Bayern, Wassertemperatur Bayern, 2020.
[94] A. Lyden, Viability of River Source Heat Pumps for District Heating, Master's Thesis, University of Strathclyde, 2015.
[95] J. Jung, J. Nam, J. Kim, et al., Estimation of temperature recovery distance and the influence of heat pump discharge on fluvial ecosystems, Water 12 (2020) 949, https://doi.org/10.3390/w12040949.
[96] P. Manz, T. Fleiter, A. Aydemir, Developing a georeferenced database of energy-intensive industry plants for estimation of excess heat potentials, eceee Summer Study Proceedings (2018) 239–247.
[97] L. Tobiasen, B. Kamuk, Waste to energy (WTE) systems for district heating, in: Waste to Energy Conversion Technology, Elsevier, 2013, pp. 120–145.
[98] S. Pezzutto, S. Zambotti, S. Croce, et al., D2.3 WP2 Report - Open Data Set for the EU28: Deliverable D2.3 Hotmaps, 2019.
[99] D. Trier, F. Bava, C.K. Skov, et al., Solar district heating - trends and possibilities: characteristics of ground-mounted systems for screening of land use requirements and feasibility, in: Subtask B Report in the IEA SHC Task 52 Programme, PlanEnergi, 2018 published by.
[100] QGIS Documentation, PyQGIS developer cookbook: v.3.22. https://docs.qgis.org/3.22/en/docs/pyqgis_developer_cookbook/index.html, 2022. (Accessed 18 August 2022).
[101] P. Manz, A. Billerbeck, M. Fallahnejad, Spatial Analysis of Renewable and Excess Heat Potentials for Climate-Neutral District Heating in Europe, Supplementary Material (2023). Available online: https://doi.org/10.24406/fordatis/280.3.
[102] C. Bernath, G. Deac, F. Sensfuß, Influence of heat pumps on renewable electricity integration: Germany in a European context, Energy Strategy Rev. 26 (2019) 100389, https://doi.org/10.1016/j.esr.2019.100389.
[103] C. Bernath, G. Deac, F. Sensfuß, Impact of sector coupling on the market value of renewable energies – a model-based scenario analysis, Appl. Energy 281 (2021) 115985, https://doi.org/10.1016/j.apenergy.2020.115985.
[104] S. Coss, V. Verda, O. Le-Corre, Multi-objective optimization of district heating network model and assessment of demand side measures using the load deviation index, J. Clean. Prod. 182 (2018) 338–351, https://doi.org/10.1016/j.jclepro.2018.02.083.
[105] D.M.Sneum, E. Sandberg, Economic incentives for flexible district heating in the Nordic countries. Int. J. Sustain. Energy Planning Manag.:27–44., dx.doi.org/10.5278/ijsepm.2018.16.3.
[106] Y. Zhang, P. Johansson, A. Sasic Kalagasidis, Assessment of district heating and cooling systems transition with respect to future changes in demand profiles and renewable energy supplies, Energy Convers. Manag. 268 (2022) 116038, https://doi.org/10.1016/j.enconman.2022.116038.
[107] H. Lund, Renewable heating strategies and their consequences for storage and grid infrastructures comparing a smart grid to a smart energy systems approach, Energy 151 (2018) 94–102, https://doi.org/10.1016/j.energy.2018.03.010.
[108] D. Fiaschi, G. Manfrida, B. Mendecka, et al., A comparison of different approaches for assessing energy outputs of combined heat and power geothermal plants, Sustainability 13 (2021) 4527, https://doi.org/10.3390/su13084527.
[109] European Commission, Background Report on EU-27 District Heating and Cooling Potentials, Barriers, Best Practice and Measures of Promotion: Report EUR 25289 EN, 2012. Luxembourg.
[110] J. Chambers, S. Zuberi, M. Jibran, et al., Spatiotemporal analysis of industrial excess heat supply for district heat networks in Switzerland, Energy 192 (2020) 116705, https://doi.org/10.1016/j.energy.2019.116705.
[111] P. Huang, B. Copertaro, X. Zhang, et al., A review of data centers as prosumers in district energy systems: renewable energy integration and waste heat reuse for district heating, Appl. Energy 258 (2020) 114109, https://doi.org/10.1016/j.apenergy.2019.114109.
[112] M. Fallahnejad, L. Kranzl, R. Haas, et al., District heating potential in the EU-27: Evaluating the impacts of heat demand reduction and market share growth, Appl. Energy 353 (2024) 122154, https://doi.org/10.1016/j.apenergy.2023.122154.
[113] Fallahnejad M District heating economic assessment (v1.0). Zenodo. https://doi.org/10.5281/zenodo.7455372.
[114] P. Stein, S. Vollnhals, Grundlagen Clusteranalytischer Verfahren, Institut für Soziologie - Universität Duisburg-Essen, 2011, p. 74.